



An adaptive PCE-HDMR metamodeling approach for high-dimensional problems

Xinxin Yue¹ · Jian Zhang¹ · Weijie Gong¹ · Min Luo² · Libin Duan³

Received: 5 October 2020 / Revised: 16 January 2021 / Accepted: 22 January 2021 / Published online: 27 February 2021
© The Author(s), under exclusive licence to Springer-Verlag GmbH, DE part of Springer Nature 2021

Abstract

Metamodel-based high-dimensional model representation (HDMR) has recently been developed as a promising tool for approximating high-dimensional and computationally expensive problems in engineering design and optimization. However, current stand-alone Cut-HDMRs usually come across the problem of prediction uncertainty while combining an ensemble of metamodels with Cut-HDMR results in an implicit and inefficient process in response approximation. To this end, a novel stand-alone Cut-HDMR is proposed in this article by taking advantage of the explicit polynomial chaos expansion (PCE) and hierarchical Cut-HDMR (named PCE-HDMR). An intelligent dividing rectangles (DIRECT) sampling method is adopted to adaptively refine the model. The novelty of the PCE-HDMR is that the proposed multi-hierarchical algorithm structure by integrating PCE with Cut-HDMR can efficiently and robustly provide simple and explicit approximations for a wide class of high-dimensional problems. An analytical function is first used to illustrate the modeling principles and procedures of the algorithm, and a comprehensive comparison between the proposed PCE-HDMR and other well-established Cut-HDMRs is then made on fourteen representative mathematical functions and five engineering examples with a wide scope of dimensionalities. The results show that the proposed PCE-HDMR has much superior accuracy and robustness in terms of both global and local error metrics while requiring fewer number of samples, and its superiority becomes more significant for polynomial-like functions, higher-dimensional problems, and relatively larger PCE degrees.

Keywords Metamodeling · Polynomial chaos expansion (PCE) · High-dimensional model representation (HDMR) · Adaptive sampling · Design optimization

1 Introduction

Metamodels (also known as surrogate models) have been widely used in the design and optimization of complex engineering systems to replace computationally expensive simulations for efficient estimation of system characteristics. Typical metamodeling techniques include polynomial response surface (PRS) (Hussain et al. 2002), radial basis

function (RBF) (Fang and Horstemeyer 2006), Kriging (KRG) (Martin and Simpson 2005), support vector regression (SVR) (Clarke et al. 2005), and ensemble of metamodels (Goel et al. 2007; Zhang et al. 2021a). Information on the comparative studies and applications of different metamodels can be found in the relevant references (e.g., Jin et al. 2001; Hussain et al. 2002; Li et al. 2010; Van Gelder et al. 2014; Ostergard et al. 2018; Parnianifard et al. 2020). Although being successful in a variety of engineering applications, it has been found that these metamodeling techniques are computationally prohibitive for solving high-dimensional problems due to the “curse of dimensionality” (Shan and Wang 2010b). With the ever-increasing complexity of engineering systems, it is very often to encounter simulation-based engineering problems of high dimensionality (e.g., larger than 10). Therefore, to effectively tackle these high-dimensional problems, an alternative metamodeling technique is demanded.

High-dimensional model representation (HDMR) has been introduced as a general set of quantitative model assessment

Responsible Editor: Erdem Acar

✉ Jian Zhang
jianzhang@u.nus.edu

¹ Department of Mechanics and Engineering Science, Jiangsu University, Zhenjiang 212013, China

² Ocean College, Zhejiang University, Zhoushan 316021, China

³ School of Automotive and Traffic Engineering, Jiangsu University, Zhenjiang 212013, China

and analysis tools for high-dimensional input-output systems (Sobol 1993; Rabitz et al. 1999; Rabitz and Alis 1999) and applied in various fields, for instance, black-box metamodeling (Li et al. 2001, 2006; Shan and Wang 2011), sensitivity analysis (Wang et al. 2017), and reliability analysis (Chowdhury and Rao 2009; Xie et al. 2017). There are mainly two types of HDMR: analysis of variance (ANOVA)-HDMR and Cut-HDMR (Rabitz and Alis 1999; Li et al. 2001). Designed for statistical purposes with the capability to identify significant variables and correlations, ANOVA-HDMR is more beneficial for sensitivity analysis, but its main disadvantage is the need to compute lots of integrals (usually by Monte Carlo summations). On the contrary, Cut-HDMR, which includes no integral computations, can exactly represent the target function by decomposing it into a set of component functions on lines, planes, and hyperplanes passing through a reference point (cut point). To this end, Cut-HDMR is more attractive in terms of modeling due to the simplicity of implementation. Nevertheless, the original Cut-HDMR model only offers a checkup table for the lack of a method to render a complete model, and an accompanying sampling strategy is also needed to support the model development.

Shan and Wang (2010a) combined RBF with Cut-HDMR to build a high-dimensional modeling approach, termed RBF-HDMR, and used an adaptive sampling method rooted in the model format. The RBF-HDMR was recently improved by Cai et al. (2016) and Liu et al. (2018). Wang et al. (2011) combined moving least squares with Cut-HDMR integrated with dividing rectangles (DIRECT) sampling method for solving high-dimensional problems. Tang et al. (2013) developed KRG-HDMR with mode pursuing sampling method and applied it to the design optimization of steel springback. The KRG-HDMR was recently enhanced and used in various optimization problems (Chen et al. 2016; Li and Wang 2016; Li et al. 2017). Huang et al. (2015) combined SVR model with Cut-HDMR to form SVR-HDMR, in which the DIRECT sampling method was also adopted, and applied it to the structure design of a heavy machine tool. Zhang et al. (2019) combined an ensemble of metamodels with Cut-HDMR for approximating high-dimensional problems. Other types of HDMR introduced by researchers include random sampling-HDMR (Li et al. 2006; Mukhopadhyay et al. 2015), hybrid HDMR (Tunga and Demiralp 2006; Chowdhury and Rao 2009), indexing-HDMR (Tunga 2011), Chebyshev-HDMR (Thomas et al. 2012), and principal component analysis (PCA)-HDMR (Hajikolaie and Wang 2014). A comparative study of different HDMRs for high-dimensional problems can be found in the relevant references, e.g., Chen et al. (2019).

The above metamodel-based HDMR approaches are promising for high-dimensional modeling. However, on one hand, stand-alone Cut-HDMR methods (e.g., RBF-HDMR, KRG-HDMR, SVR-HDMR) may come across problems with

prediction uncertainty, meaning that one Cut-HDMR metamodel may be suitable for a problem but unsuitable for another. On the other hand, although combining an ensemble of metamodels with Cut-HDMR (e.g., Zhang et al. 2019) can overcome the difficulty of prediction uncertainty for different problems, it cannot provide simple and explicit expression for a black-box problem, and predicting the responses of unobserved points will become very slow and complex due to the involvement of numerous parameters of different metamodels (e.g., the polynomial coefficients in the PRS, interpolation coefficients in the RBF, and parameters used for the correlation function in the KRG, which are all needed to be determined if PRS, RBF, and KRG are formed into an ensemble of metamodels) in representing Cut-HDMR. To this end, there is a gap/need to develop an efficient and robust HDMR metamodeling approach which can provide simple and explicit expression for a wide class of high-dimensional problems.

Motivated by the preceding analysis, this article proposes a novel metamodeling approach based on the integration of polynomial chaos expansion (PCE) and Cut-HDMR (PCE-HDMR) in order to obtain a simple, accurate, and robust approximation for high-dimensional problems. The PCE approach is to represent explicitly the model response as a series of orthonormal multivariate polynomials, i.e., polynomial chaos (PC) basis (Ghanem and Spanos 1991; Xiu and Karniadakis 2002), and has received much attention for uncertainty and sensitivity analyses (Sudret 2008; Lee and Chen 2009; Cheng et al. 2020; Zhang et al. 2021b). Therefore, response quantification in the context of PCE is equivalent to estimation of the PC coefficients that are the coordinates of model response in the basis and can be evaluated at a set of sampling points in the input space. It is worth noting that, although orthonormal basis functions are used in both the proposed PCE-HDMR and existing PCA-HDMR (Hajikolaie and Wang 2014), these two methods are fundamentally different: (1) PCA-HDMR belongs to ANOVA-HDMR, whereas PCE-HDMR is a Cut-HDMR; (2) PCA-HDMR identifies the appropriate combinations of orthonormal basis functions for model approximation along the direction of the last HDMR principal component with minimum variation (or with weighted combinations of different component PCA-HDMR models). Nevertheless, the proposed PCE-HDMR decomposes the model response into a series of component functions on lines, planes, and hyperplanes passing through a cut point and further expands the respective components in terms of multivariate orthonormal polynomials. Due to the algorithm structure of multiple hierarchies that are successively produced by the Cut-HDMR and PCE, the proposed PCE-HDMR represents the correlation among inputs with an explicit model of finite terms (up to second-order) and quantifies the output response by evaluating the PC coefficients in regard to the selected orthonormal polynomials. By this way, the proposed approach overcomes the

aforementioned gap with combination of the DIRECT sampling method. Therefore, compared to the existing studies, the main contribution of this paper is that by integrating PCE with Cut-HDMR to form a multi-hierarchical algorithm structure, the proposed PCE-HDMR can efficiently and robustly provide simple and explicit approximations for a wide class of high-dimensional problems.

The remainder of this article is organized as follows. Section 2 presents the theoretical bases of HDMR and PCE. An adaptive PCE-HDMR metamodeling approach is proposed in Section 3. Section 4 evaluates the performance of PCE-HDMR with extensive numerical experiments. Concluding remarks are summarized in Section 5.

2 Theoretical bases

2.1 HDMR

A general HDMR model for the output response $f(\mathbf{x})$ can be expressed in a hierarchical correlated function expansion in terms of an n -dimensional input vector $\mathbf{x} = [x_1, x_2, \dots, x_n]^T \in \mathbb{R}^n$ as

$$\begin{aligned} f(\mathbf{x}) = & f_0 + \sum_{1 \leq i \leq n} f_i(x_i) + \sum_{1 \leq i < j \leq n} f_{ij}(x_i, x_j) \\ & + \sum_{1 \leq i < j < k \leq n} f_{ijk}(x_i, x_j, x_k) + \dots \\ & + \sum_{1 \leq i_1 < \dots < i_l \leq n} f_{i_1 i_2 \dots i_l}(x_{i_1}, x_{i_2}, \dots, x_{i_l}) + \dots \\ & + f_{12 \dots n}(x_1, x_2, \dots, x_n) \end{aligned} \quad (1)$$

where f_0 is a constant term denoting the zeroth-order effect on $f(\mathbf{x})$, $f_i(x_i)$ is a first-order term expressing the effect of variable x_i acting independently upon $f(\mathbf{x})$, $f_{ij}(x_i, x_j)$ is a second-order term that describes the correlated effect of variables x_i and x_j on $f(\mathbf{x})$ after removing their individual contributions, the higher-order terms give the effects of increasing numbers of correlated variables acting together on $f(\mathbf{x})$, and the last term $f_{12 \dots n}(x_1, x_2, \dots, x_n)$ represents the residual effect of all input variables acting together on $f(\mathbf{x})$ after all the lower-order correlations and individual influences have been removed. For most physical systems, the higher-order terms in Eq. (1) are negligible, and only lower-order correlations among input variables are expected to have a significant influence on the output response (Rabitz and Alis 1999). In this regard, the second-order HDMR expansion is widely used, and this would dramatically reduce the required computational cost while providing an acceptable modeling accuracy when one seeks to map input-output relationships of complex physical systems.

Among the developed HDMRs (Li et al. 2001; Li et al. 2006; Tunga and Demiralp 2006), the Cut-HDMR (Rabitz

and Alis 1999) presents a simple and cost-efficient model structure and provides a comparable accuracy to other HDMRs. Therefore, the Cut-HDMR is chosen as the basis for the proposed PCE-HDMR. The Cut-HDMR expansion is an exact representation of the output $f(\mathbf{x})$ by a superposition of its values on the cuts (cut lines, planes, and hyperplanes) passing through a cut point $\mathbf{x}_0 = [x_{10}, x_{20}, \dots, x_{n0}]^T$ in the input variable space. As a result, the component functions of Cut-HDMR in Eq. (1) can be expressed as

$$f_0 = f(\mathbf{x}_0) \quad (2)$$

$$f_i(x_i) = f(x_i, \mathbf{x}_0^i) - f_0 \quad (3)$$

$$f_{ij}(x_i, x_j) = f(x_i, x_j, \mathbf{x}_0^{ij}) - f_i(x_i) - f_j(x_j) - f_0 \quad (4)$$

$$\begin{aligned} & f_{ijk}(x_i, x_j, x_k) \\ &= f(x_i, x_j, x_k, \mathbf{x}_0^{ijk}) - f_{ij}(x_i, x_j) - f_{ik}(x_i, x_k) - f_{jk}(x_j, x_k) \\ & \quad - f_i(x_i) - f_j(x_j) - f_k(x_k) - f_0 \end{aligned} \quad (5)$$

...

$$\begin{aligned} & f_{12 \dots n}(x_1, x_2, \dots, x_n) \\ &= f(\mathbf{x}) - f_0 - \sum_i f_i(x_i) - \sum_{ij} f_{ij}(x_i, x_j) - \dots \end{aligned} \quad (6)$$

where $\mathbf{x}_0^i, \mathbf{x}_0^{ij}$, and \mathbf{x}_0^{ijk} are \mathbf{x}_0 without elements x_i , (x_i, x_j) , and (x_i, x_j, x_k) , respectively. The points \mathbf{x}_0 , $(x_i, \mathbf{x}_0^i) = [x_{10}, x_{20}, \dots, x_i, \dots, x_{n0}]^T$, and $(x_i, x_j, \mathbf{x}_0^{ij}) = [x_{10}, x_{20}, \dots, x_i, \dots, x_j, \dots, x_{n0}]^T$ are referred as the zeroth-order, first-order, and second-order points, respectively. Accordingly, $f(\mathbf{x}_0)$, $f(x_i, \mathbf{x}_0^i)$, and $f(x_i, x_j, \mathbf{x}_0^{ij})$ are respectively the values of $f(\mathbf{x})$ at points \mathbf{x}_0 , (x_i, \mathbf{x}_0^i) , and $(x_i, x_j, \mathbf{x}_0^{ij})$, while $f_i(x_i)$ is the first-order component output response at x_i along the i -th cut line and $f_{ij}(x_i, x_j)$ is the second-order component output response at (x_i, x_j) on the i - j cut plane.

Although Cut-HDMR has shown good properties, the model given in Eqs. (2)–(6) only offers a checkup table and cannot be used for data interpolation at its current stage. To have a complete and available model, this study proposes to adopt PCE as the basis to build the component functions of Cut-HDMR.

2.2 PCE

The classic PCE of the model response $y = f(\mathbf{x})$ can be represented as follows:

$$y = f(\mathbf{x}) = \sum_{\alpha \in \mathbb{N}^n} \beta_\alpha \psi_\alpha(\mathbf{x}) \quad (7)$$

where $\alpha = (\alpha_1, \dots, \alpha_n)$ (with $\alpha_i \geq 0$) is an n -dimensional index, $\{\beta_\alpha : \alpha \in \mathbb{N}^n\}$ are unknown deterministic PC coefficients, and $\{\psi_\alpha : \alpha \in \mathbb{N}^n\}$ are multivariate orthonormal

polynomials. Assuming that the input vector \mathbf{x} has independent components x_i with prescribed probability density function (PDF) $f_{X_i}(x_i)$, the input joint PDF can be obtained by

$$f_{\mathbf{x}}(\mathbf{x}) = \prod_{i=1}^n f_{X_i}(x_i) \quad (8)$$

For each input x_i ($i = 1, \dots, n$), a family of univariate orthogonal polynomials $(\pi_{\alpha_i}^{(1)}(x_i), \pi_{\alpha_i}^{(2)}(x_i), \dots)$ can be constructed with respect to $f_{X_i}(x_i)$ satisfying

$$\mathbb{E}[\pi_{\alpha_i}^{(j)}(x_i) \pi_{\alpha_i}^{(k)}(x_i)] = \int_{X_i} \pi_{\alpha_i}^{(j)}(x_i) \pi_{\alpha_i}^{(k)}(x_i) f_{X_i}(x_i) dx_i = c_{\alpha_i}^{(j,k)} \delta^{(j,k)} \quad (9)$$

where $\delta^{(j,k)}$ is the Kronecker symbol with $\delta^{(j,k)} = 1$ if $j = k$, otherwise $\delta^{(j,k)} = 0$, and $c_{\alpha_i}^{(j,k)}$ is a constant. Different types of univariate orthogonal polynomials commonly used for constructing PC can be found in the literature, e.g., Xiu and Karniadakis (2002). The univariate polynomials are usually normalized as

$$\psi_{\alpha_i}^{(j)} = \pi_{\alpha_i}^{(j)}(x_i) / \sqrt{c_{\alpha_i}^{(j,j)}} \quad (10)$$

By tensorizing the resulting n families of univariate polynomials, one can obtain the multivariate polynomial:

$$\psi_{\alpha}(\mathbf{x}) = \prod_{i=1}^n \psi_{\alpha_i}^{(i)}(x_i) \quad (11)$$

In practice, the PCE in Eq. (7) is usually truncated for computational purposes. A common way is to retain those polynomials whose total degree $|\alpha| = \sum_{i=1}^n \alpha_i$ does not exceed a given degree of p :

$$y \approx f_p(\mathbf{x}) = \sum_{\alpha \in \mathcal{A}^{p,n}} \beta_{\alpha} \psi_{\alpha}(\mathbf{x}), \quad \mathcal{A}^{p,n} = \{\alpha \in \mathbb{N}^n : |\alpha| \leq p\} \quad (12)$$

The expression of Eq. (12) is called the full PCE of degree p of the model response y . The total number of unknown PC coefficients P can be calculated from the maximum degree p and the dimensionality n of inputs as follows:

$$P = \binom{n+p}{p} = \frac{(n+p)!}{n!p!} \quad (13)$$

With such a truncation, the problem of characterizing the model response y is converted into computing a finite set of unknown PC coefficients.

In order to compute the PC coefficients, nonintrusive regression-based techniques (Sudret 2008; Szepietowska et al. 2018; Zhang et al. 2021b) are often used to seek a PCE that satisfies:

$$f_p(x_j) = \sum_{\alpha \in \mathcal{A}^{p,n}} \beta_{\alpha} \psi_{\alpha}(x_j) \approx f(x_j) = y_j, \quad j = 1, \dots, N \quad (14)$$

where N is the number of input-output samples. Equation (14) can be rewritten in the form of $\mathbf{y} = \psi \beta$, where $\beta \in \mathbb{R}^P$ is a vector of unknown PC coefficients, $\mathbf{y} \in \mathbb{R}^N$ is a vector of N realizations of the model output, and $\psi \in \mathbb{R}^{N \times P}$ is the measurement matrix of which each column contains evaluations of the PC basis polynomials at the N samples. The PC coefficients are evaluated by minimizing the residual between the model response and PCE approximation. For $N \geq P$, the unknown coefficients can be computed using the least-squares regression: $\beta = (\psi^T \psi)^{-1} \psi^T \mathbf{y}$. When $N < P$, the system equation for β becomes ill-posed, and the least-squares approach is no longer feasible. To this end, some form of constraint or regularization is usually introduced to identify a unique solution.

From the theory of compressed sensing (Donoho 2006; Tropp and Gilbert 2007; Eldar and Kutyniok 2012), it is indicated that the model responses can be accurately reconstructed for problems where the quantity of interest demonstrates stochastic sparsity. In the context of the PCE, this sparsity allows the unknown coefficients in Eq. (14) to be determined with only a few terms of significant nonzeros when the number of samples is less than the dimensionality of the PC coefficients, i.e., $N \ll P$. For a PCE with sufficient sparsity, the significant nonzero coefficients can be obtained by solving the following ℓ_1 -minimization problem

$$\min_{\beta \in \mathbb{R}^P} \|\beta\|_1 \quad \text{subject to} \quad \|\psi \beta - \mathbf{y}\|_2 \leq \epsilon \quad (15)$$

with an ℓ_2 norm constraint to account for the error ϵ in the p -th degree truncation of the PCE. Equation (15) can be solved by two main categories of approaches: basis pursuit (Chen et al. 1998) and greedy algorithms (Tropp and Gilbert 2007; Baptista et al. 2019). In the present paper, a greedy algorithm, orthogonal matching pursuit (OMP), is adopted to obtain a sparse PCE as the basis for constructing the component functions of Cut-HDMR. To this end, it is now possible to introduce a simple, accurate, and robust algorithm for modeling high-dimensional problems.

3 An adaptive PCE-HDMR metamodeling approach

In this section, an adaptive PCE-HDMR is proposed in order to improve the accuracy and robustness of the HDMR. Firstly, the principle for model construction is described. Then, an intelligent sampling method called DIRECT sampling is introduced. The procedure for building an adaptive PCE-HDMR is subsequently elaborated, and an example to illustrate the detailed steps of the proposed algorithm is finally presented.

3.1 Principle of PCE-HDMR

In the process of metamodeling, since the characteristics of underlying functions or problems are usually not known a priori, it is very challenging to select the most appropriate metamodel for a specific application. Due to this issue, most existing Cut-HDMR metamodels such as RBF-HDMR, KRG-HDMR, and SVR-HDMR usually encounter the situation of prediction uncertainty for different problems. On the other hand, although the ensemble of metamodels can provide robust prediction for a variety of problems, its integration with Cut-HDMR usually involves lots of different metamodel parameters that are usually determined by using optimization algorithms and thus leads to a complex and inefficient process with an implicit expression in predicting the responses. The proposed PCE-HDMR model makes use of the hierarchical structure of HDMR and employs the PCE metamodel in an explicit expansion of multivariate orthonormal polynomials to construct the component functions of Cut-HDMR. Therefore, Eqs. (2)–(6) can be rewritten as follows:

$$f_0 = f(\mathbf{x}_0) \quad (16)$$

$$\hat{f}_i(x_i) = \sum_{\alpha \in \mathcal{A}^{p,1}} \beta_\alpha \psi_\alpha(x_i, \mathbf{x}_0^i) \quad (17)$$

$$\hat{f}_{ij}(x_i, x_j) = \sum_{\alpha \in \mathcal{A}^{p,2}} \beta_\alpha \psi_\alpha(x_i, x_j, \mathbf{x}_0^{ij}) \quad (18)$$

$$\hat{f}_{ijk}(x_i, x_j, x_k) = \sum_{\alpha \in \mathcal{A}^{p,3}} \beta_\alpha \psi_\alpha(x_i, x_j, x_k, \mathbf{x}_0^{ijk}) \quad (19)$$

$$\hat{f}_{12 \dots n}(x_1, x_2, \dots, x_n) = \sum_{\alpha \in \mathcal{A}^{p,n}} \beta_\alpha \psi_\alpha(x_1, x_2, \dots, x_n) \quad (20)$$

where the one-dimensional (1D) PCE model $\hat{f}_i(x_i)$ is the approximation of the first-order component response $f_i(x_i)$, the two-dimensional (2D) PCE model $\hat{f}_{ij}(x_i, x_j)$ is the approximation of the second-order component response $f_{ij}(x_i, x_j)$, and so on. Referred as the modeling lines, planes, and hyperplanes, Eqs. (16)–(20) are substituted into the HDMR in Eq. (1), and we have the following formulation:

$$\begin{aligned} f(\mathbf{x}) \cong & f_0 + \sum_{1 \leq i \leq n} \sum_{\alpha \in \mathcal{A}^{p,1}} \beta_\alpha \psi_\alpha(x_i, \mathbf{x}_0^i) + \sum_{1 \leq i < j \leq n} \sum_{\alpha \in \mathcal{A}^{p,2}} \beta_\alpha \psi_\alpha(x_i, x_j, \mathbf{x}_0^{ij}) \\ & + \sum_{1 \leq i < j < k \leq n} \sum_{\alpha \in \mathcal{A}^{p,3}} \beta_\alpha \psi_\alpha(x_i, x_j, x_k, \mathbf{x}_0^{ijk}) + \dots \\ & + \sum_{1 \leq i_1 < \dots < i_l \leq n} \sum_{\alpha \in \mathcal{A}^{p,l}} \beta_\alpha \psi_\alpha(x_{i_1}, \dots, x_{i_l}, \mathbf{x}_0^{i_1 \dots i_l}) + \dots \\ & + \sum_{\alpha \in \mathcal{A}^{p,n}} \beta_\alpha \psi_\alpha(x_1, x_2, \dots, x_n) \end{aligned} \quad (21)$$

The expression of Eq. (21) is called the full PCE-HDMR, which approximates the output in a multi-hierarchical way: the first hierarchy is that the output is represented by

superposing its values on the cut lines, planes, and hyperplanes with reference to a cut point, and the second hierarchy is that the component outputs of different orders resulting from the first hierarchy are further expanded in terms of multivariate orthonormal polynomials. To this end, PCE-HDMR distinctly represents the correlation among input variables with an explicit model of finite terms and quantifies the output response by estimating the PC coefficients with respect to the selected orthonormal polynomials.

As described in Section 2, a second-order HDMR expansion is usually sufficient to represent the original model. Therefore, the PCE-HDMR can be truncated as:

$$f(\mathbf{x}) \approx f_0 + \sum_{1 \leq i \leq n} \sum_{\alpha \in \mathcal{A}^{p,1}} \beta_\alpha \psi_\alpha(x_i, \mathbf{x}_0^i) + \sum_{1 \leq i < j \leq n} \sum_{\alpha \in \mathcal{A}^{p,2}} \beta_\alpha \psi_\alpha(x_i, x_j, \mathbf{x}_0^{ij}) \quad (22)$$

The number of unknown PC coefficients in the second-order PCE-HDMR is given by

$$P^{\text{PCE-HDMR}} = n * P^{(i)} + \frac{n(n-1)}{2} * P^{(ij)} \quad (23)$$

where $P^{(i)} = \frac{(p_1+1)!}{p_1!1!}$ and $P^{(ij)} = \frac{(p_2+2)!}{p_2!2!}$ are the numbers of PC coefficients in the 1D PCE model $\hat{f}_i(x_i)$ with the PCE degree of p_1 and 2D PCE model $\hat{f}_{ij}(x_i, x_j)$ with the PCE degree of p_2 , respectively. Comparing Eq. (23) with Eq. (13), it is observed that PCE-HDMR dramatically reduces the number of model evaluations (i.e., the computational cost) required for computing the PC coefficients by transforming an exponentially increasing computational difficulty into a polynomial one. To further reduce the modeling cost, an intelligent sampling method is adopted in the sequel.

3.2 DIRECT sampling method

As a pattern search method that keeps a tradeoff between global and local search, the DIRECT algorithm was developed to handle global optimization problems with bound constraints (Jones et al. 1993). It is capable of identifying the area near a global minimum within few function evaluations. On the other hand, the advantage of the HDMR is to utilize a limited number of sample points to construct the metamodel for approximating the assigned problem. If the area near a global minimum is located, the metamodel can be built within this area. Therefore, the original design space is actually reduced.

It is also noticed that the DIRECT algorithm is a deterministic sampling method, which is mainly to find all the local extreme points in order to locate the global minimum points in different parameters within the search ranges. This method has a very fast convergence rate and is robust to local optimum. Therefore, the DIRECT sampling method is more appropriate for the HDMR and used in this study to construct the PCE-

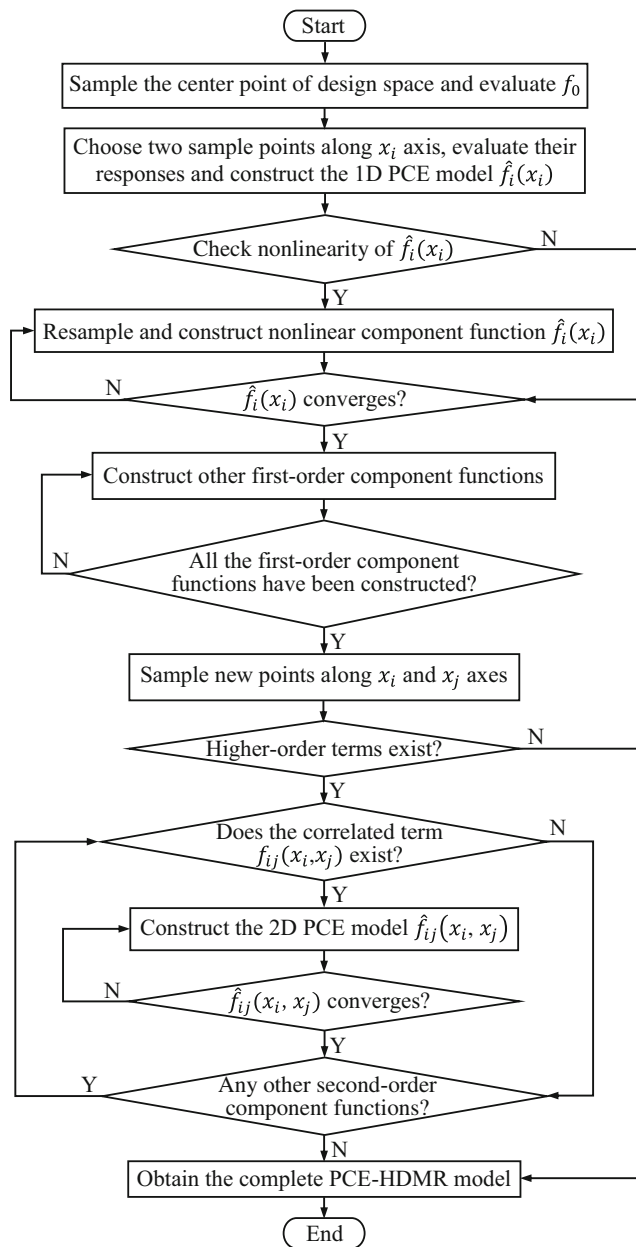


Fig. 2 The flowchart of the adaptive PCE-HDMR

$(x_i^{upper}, x_0^i) - f_0$ and $f_i(x_i^{lower}) = f(x_i^{lower}, x_0^i) - f_0$; and construct the 1D PCE model $\hat{f}_i(x_i)$.

- Check the linearity of the first-order component function $\hat{f}_i(x_i)$ constructed in Step 2. Randomly generate a sample point x_i^{rand} along x_i axis, and evaluate the response value $f_i(x_i^{rand}) = f(x_i^{rand}, x_0^i) - f_0$. If $\left\| \frac{\hat{f}_i(x_i^{rand}) - f_i(x_i^{rand})}{f_i(x_i^{rand})} \right\| \leq \varepsilon_1$ and $\left\| \frac{f_i(x_i^{upper}) - \hat{f}_i(x_i)}{x_i^{upper} - x_i} - \frac{\hat{f}_i(x_i) - f_i(x_i^{lower})}{x_i - x_i^{lower}} \right\| \leq \varepsilon_1$, where ε_1 is a threshold, $\hat{f}_i(x_i)$ is considered as linear, and the construction of the i -th function is completed. Otherwise, add $(x_{i0}, f_i(x_{i0}))$ to the existing input-output samples

$\{(x_i^{upper}, f_i(x_i^{upper})), (x_i^{lower}, f_i(x_i^{lower}))\}$, and reconstruct the PCE model $\hat{f}_i(x_i)$.

- Resample along x_i axis using the DIRECT sampling method, and check the convergence of the component function $\hat{f}_i(x_i)$. First, select the optimal side (i.e., the optimal hyper-rectangle in 1D) with the maximum response difference between its end points, i.e., $\max(|f_i(x_{i0}) - f_i(x_i^{lower})|, |f_i(x_i^{upper}) - f_i(x_{i0})|)$, and sample a new point x_i^{new} at one-third of the side from its end point of larger response (absolute) value. If the convergence criterion $\left\| \frac{\hat{f}_i(x_i^{new}) - f_i(x_i^{new})}{f_i(x_i^{new})} \right\| \leq \varepsilon_1$ is not satisfied, add $(x_i^{new}, f_i(x_i^{new}))$ to the existing samples, update the PCE model $\hat{f}_i(x_i)$, and resume Step 4. Otherwise, continue to select the optimal side with the maximum length, i.e., $\max(|x_{i0} - x_i^{lower}|, |x_i^{upper} - x_{i0}|)$: (1) if the optimal side based on the maximum length is the same as that based on the maximum response difference, add $(x_i^{new}, f_i(x_i^{new}))$ to the existing samples, update the PCE model $\hat{f}_i(x_i)$, and resume Step 4; (2) otherwise, sample another new point in a similar way as above for the optimal side based on the maximum length. If the convergence criterion is fulfilled, terminate the i -th function construction. If not, add this new point to the existing samples, update the PCE model $\hat{f}_i(x_i)$, and resume Step 4.
- Repeat from Step 2 to Step 4 until all the first-order component functions are constructed. To this end, the first-order PCE-HDMR model is completed.

- Form a new point (x_i, x_j, x_0^{ij}) by randomly combining point values sampled in Step 2 to Step 5, and evaluate its response $f(x_i, x_j, x_0^{ij})$. If

$\left\| \frac{f(x_i, x_j, x_0^{ij}) - \hat{f}_i(x_i) - \hat{f}_j(x_j) - f_0}{f(x_i, x_j, x_0^{ij})} \right\| \leq \varepsilon_1$, where $\hat{f}_i(x_i)$ and $\hat{f}_j(x_j)$ are calculated based on the first-order PCE-HDMR models obtained in Step 4 to Step 5, it is considered that there is no higher-order HDMR component function and the construction process in this term terminates. Otherwise, go to the next step.

- Choose four sample points by combining point values respectively at the lower and upper limits of the range of variables x_i and x_j , i.e., $(x_i^{lower}, x_j^{lower}, x_0^j)$, $(x_i^{lower}, x_j^{upper}, x_0^j)$, $(x_i^{upper}, x_j^{lower}, x_0^j)$, and $(x_i^{upper}, x_j^{upper}, x_0^j)$; evaluate their responses; and construct the 2D PCE model $\hat{f}_{ij}(x_i, x_j)$. Generate a new point $(x_i^{new}, x_j^{new}, x_0^{ij})$ similarly as in Step 6, and check the convergence criterion $\left\| \frac{\hat{f}_{ij}(x_i^{new}, x_j^{new}) - f_{ij}(x_i^{new}, x_j^{new})}{f_{ij}(x_i^{new}, x_j^{new})} \right\| \leq \varepsilon_1$. If the

convergence criterion is satisfied, the construction of $\hat{f}_{ij}(x_i, x_j)$ is completed. Otherwise, add this new point to the existing sample points, reconstruct the PCE model $\hat{f}_{ij}(x_i, x_j)$, generate another new point as in Step 6, and check the above convergence criterion. Repeat this process until $\hat{f}_{ij}(x_i, x_j)$ converges.

8. In a similar manner, construct the 2D PCE model for all pairs of input variables. Finally, the complete PCE-HDMR model is obtained

$$\hat{f}(\mathbf{x}) = f_0 + \sum_{1 \leq i \leq n} \hat{f}_i(x_i) + \sum_{1 \leq i < j \leq n} \hat{f}_{ij}(x_i, x_j) \quad (26)$$

3.4 An example for adaptive PCE-HDMR

For better illustrating the PCE-HDMR modeling process, consider the following analytical function of three variables:

$$f(\mathbf{x}) = (x_1 - 1)^2 + (x_1 - x_2)^2 + x_2 x_3 + 0.5, \mathbf{x} \in [0, 1]^3 \quad (27)$$

This function has linear and quadratic responses along variables x_1 and x_2 , linear responses along variable x_3 , and two pairs of correlated variables, i.e., x_1 and x_2 and x_2 and x_3 . It is assumed that the analytical function is a black-box problem with unknown expression, and a corresponding output can be determined by experiment for a given set of input variables. Therefore, an approximate model for Eq. (27) can be constructed step by step using the proposed PCE-HDMR method:

1. Select the center point $\mathbf{x}_0 = [0.5, 0.5, 0.5]^T$ of the design space as the cut point, and obtain the corresponding response by experiment:

$$f_0 = f(\mathbf{x}_0) = 1 \quad (28)$$

2. Sample two points along x_1 axis and respectively at its upper and lower limits, i.e., $(x_1^{upper}, \mathbf{x}_0^1) = [1, 0.5, 0.5]^T$ and $(x_1^{lower}, \mathbf{x}_0^1) = [0, 0.5, 0.5]^T$; get the corresponding responses by experiment: $f(x_1^{upper}, \mathbf{x}_0^1) = 1$ and $f(x_1^{lower}, \mathbf{x}_0^1) = 2$; and obtain $f_1(x_1^{upper}) = f(x_1^{upper}, \mathbf{x}_0^1) - f_0 = 0$ and $f_1(x_1^{lower}) = f(x_1^{lower}, \mathbf{x}_0^1) - f_0 = 1$. Then, the first-order component function $\hat{f}_1(x_1)$ can be constructed by PCE-HDMR with $\{(1, 0), (0, 1)\}$: $\hat{f}_1(x_1) = \beta_0 L_0(x_1) + \beta_1 L_1(x_1)$, where the PC coefficients β_0 and β_1 are obtained by the OMP algorithm with $\beta_0 = \frac{1}{2}$ and $\beta_1 = -\frac{1}{2}$. The Legendre polynomials $L_n(x)$ are orthogonal with respect to the uniform probability measure over $[-1, 1]$ and may be generated by the recurrence relationship (Sudret 2008):

$$L_0(x) = 1 \\ (n+1)L_{n+1}(x) = (2n+1)xL_n(x) - nL_{n-1}(x) \quad (29)$$

For example, the first three Legendre polynomials are $L_1(x) = x$, $L_2(x) = \frac{1}{2}(3x^2 - 1)$, and $L_3(x) = \frac{1}{2}(5x^3 - 3x)$. Therefore, $\hat{f}_1(x_1) = \frac{1}{2}(1 - x_1)$, $x_1 \in [-1, 1]$. Transforming the design space of variable x_1 from $[-1, 1]$ to $[0, 1]$, we will have $\hat{f}_1(x_1) = 1 - x_1$.

3. Randomly generate a sample point $(x_1^{rand}, \mathbf{x}_0^1) = [0.4284, 0.5, 0.5]^T$ along x_1 axis, get the corresponding response by experiment: $f(x_1^{rand}, \mathbf{x}_0^1) = 1.0819$, and obtain $f_1(x_1^{rand}) = f(x_1^{rand}, \mathbf{x}_0^1) - f_0 = 0.0819$. Check the linearity of the first-order component function $\hat{f}_1(x_1)$ with

$$\varepsilon_1 = 0.001: \left\| \frac{\hat{f}_1(x_1^{rand}) - \hat{f}_1(x_1^{rand})}{f_1(x_1^{rand})} \right\| = 5.9792 > \varepsilon_1, \text{ and } \left\| \frac{f_1(x_1^{upper}) - \hat{f}_1(x_1^0)}{1 - 0.5} - \frac{\hat{f}_1(x_1^0) - f_1(x_1^{lower})}{0.5 - 0} \right\| = 0 < \varepsilon_1. \text{ Therefore,}$$

$\hat{f}_1(x_1)$ is nonlinear. Add $(0.5, 0)$ to the existing input-output samples $\{(1, 0), (0, 1)\}$, and obtain the reconstructed PCE model $\hat{f}_1(x_1) = 2x_1^2 - 3x_1 + 1$.

4. Select the optimal side $[0, 0.5]$ based on the maximum response difference, and generate a new sample $(\frac{1}{6}, \frac{5}{9})$ according to the DIRECT sampling method. The convergence criterion is satisfied: $\left\| \frac{\hat{f}_1(\frac{1}{6}) - f_1(\frac{1}{6})}{f_1(\frac{1}{6})} \right\| = 0 \leq \varepsilon_1$. Since the side $[0, 0.5]$ is also optimal based on the maximum length, add $(\frac{1}{6}, \frac{5}{9})$ to the existing samples, and get the updated PCE model $\hat{f}_1(x_1) = 2x_1^2 - 3x_1 + 1$. Then, select the next optimal side $[\frac{1}{6}, \frac{1}{2}]$ based on the maximum response difference, similarly generate another new sample $(\frac{5}{18}, \frac{26}{81})$, and find that $\left\| \frac{\hat{f}_1(\frac{5}{18}) - f_1(\frac{5}{18})}{f_1(\frac{5}{18})} \right\| = 0 \leq \varepsilon_1$. Continue to select the optimal side $[\frac{1}{2}, 1]$ based on the maximum length, and obtain the next new sample $(\frac{2}{3}, -\frac{1}{9})$. Since $\left\| \frac{\hat{f}_1(\frac{2}{3}) - f_1(\frac{2}{3})}{f_1(\frac{2}{3})} \right\| = 0 \leq \varepsilon_1$, the construction of $\hat{f}_1(x_1)$ is completed. We can get:

$$\hat{f}_1(x_1) = 2x_1^2 - 3x_1 + 1 \equiv f_1(x_1) \quad (30)$$

5. Repeat the above Step 2 to Step 4 along x_2 and x_3 axes, respectively, and we can get:

$$\hat{f}_2(x_2) = x_2^2 - \frac{x_2}{2} \equiv f_2(x_2) \quad (31)$$

$$\hat{f}_3(x_3) = \frac{x_3}{2} - \frac{1}{4} \equiv f_3(x_3) \quad (32)$$

6. Form a new point $(x_1^{upper}, x_2^{upper}, x_0^{12}) = [1, 1, 0.5]^T$, by randomly combining point values sampled in Step 2 to Step 5, get the corresponding response by experiment: $f(x_1^{upper}, x_2^{upper}, x_0^{12}) = 1$, and calculate $\hat{f}_1(x_1^{upper}) = 0$ and $\hat{f}_2(x_2^{upper}) = 0.5$ using the first-order PCE-HDMR model obtained in Eqs. (30)–(32). Check whether there is higher-order HDMR component function with $\varepsilon_1 = 0.001$:

$$\left\| \frac{f(x_1^{upper}, x_2^{upper}, x_0^{12}) - \hat{f}_1(x_1^{upper}) - \hat{f}_2(x_2^{upper}) - f_0}{f(x_1^{upper}, x_2^{upper}, x_0^{12})} \right\| = 0.5 > \varepsilon_1.$$

7. Therefore, it is deemed that there exists correlation between x_1 and x_2 . Choose four sample points $\{[0, 0, 0.5]^T, [0, 1, 0.5]^T, [1, 0, 0.5]^T, [1, 1, 0.5]^T\}$ respectively at the lower and upper limits of the range of x_1 and x_2 , evaluate their responses, and construct the second-order component function

$$\hat{f}_{12}(x_1, x_2) = -\frac{1}{2}L_1(x_1)L_2(x_2) = -\frac{1}{2}x_1x_2, x_1, x_2 \in [-1, 1].$$

Transforming the design space of variables x_1 and x_2 from $[-1, 1]^2$ to $[0, 1]^2$, we will have

$$\hat{f}_{12}(x_1, x_2) = x_1 + x_2 - 2x_1x_2 - \frac{1}{2}.$$

Generate a new point $[\frac{5}{18}, 0, 0.5]^T$ as in Step 6, and find that the convergence

$$\left\| \frac{\hat{f}_{12}(x_1, x_2) - f_{12}(x_1, x_2)}{f_{12}(x_1, x_2)} \right\| \leq \varepsilon_1 \text{ is satisfied. Therefore,}$$

terminate the construction of $\hat{f}_{12}(x_1, x_2)$, and we can get

$$\hat{f}_{12}(x_1, x_2) = x_1 + x_2 - 2x_1x_2 - \frac{1}{2} \equiv f_{12}(x_1, x_2) \quad (33)$$

8. Repeat the above Step 6 to Step 7 to construct the second-order HDMR component functions for all pairs of input variables. We can get that there is no component function $\hat{f}_{13}(x_1, x_3)$, and

$$\hat{f}_{23}(x_2, x_3) = -\frac{x_2}{2} - \frac{x_3}{2} + x_2x_3 + \frac{1}{4} \equiv f_{23}(x_2, x_3) \quad (34)$$

9. By substituting Eqs. (28) and (30)–(34) into Eq. (26), the PCE-HDMR model for approximating the analytical function (27) is finally obtained:

$$\hat{f}(\mathbf{x}) = (x_1 - 1)^2 + (x_1 - x_2)^2 + x_2x_3 + 0.5 \equiv f(\mathbf{x}) \quad (35)$$

It is found that not only the PCE-HDMR model (35) but also its component functions, i.e., Eqs. (30)–(34), are the same as their analytical expressions, meaning that the proposed PCE-HDMR can exactly reproduce the mathematical function of second-order polynomials at both component and whole

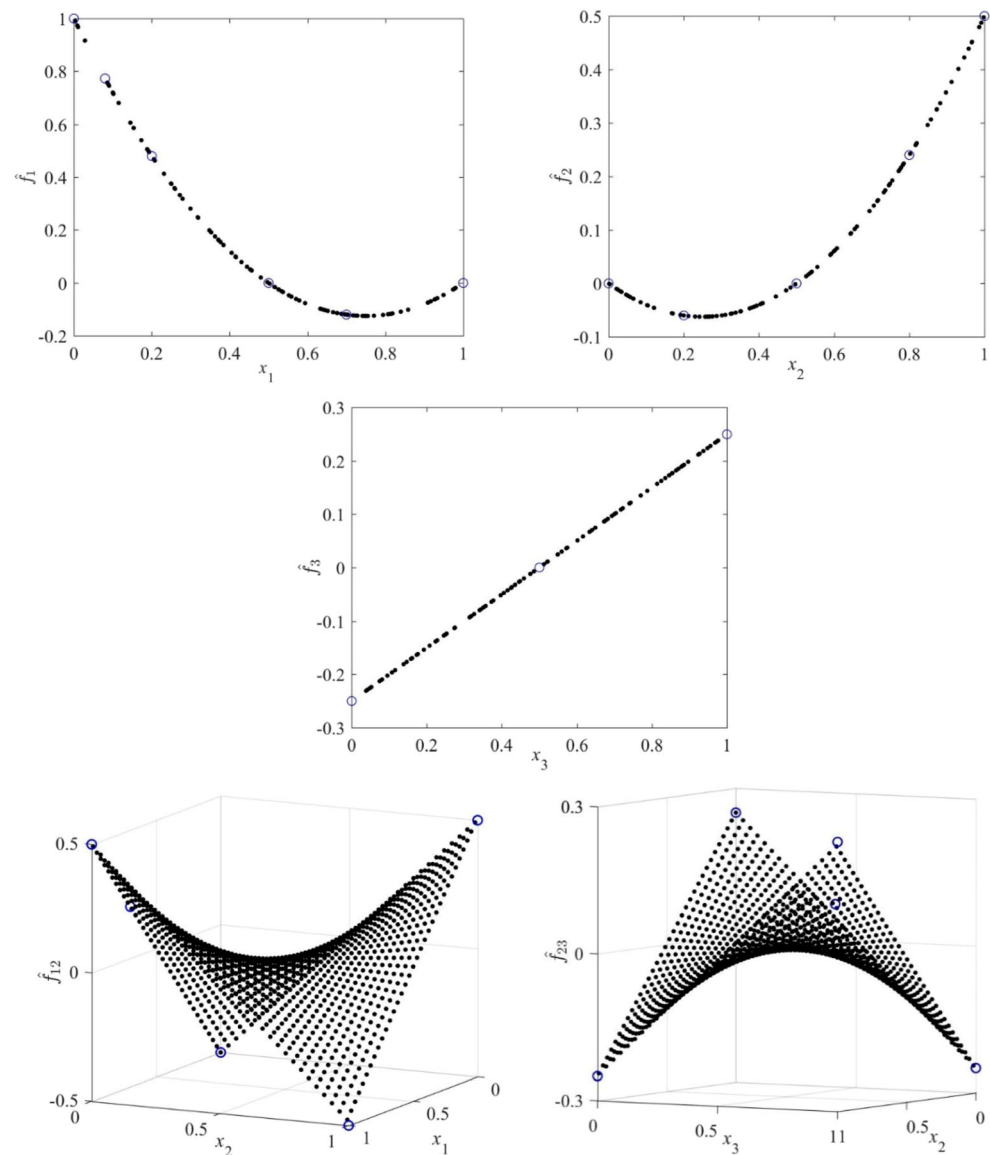
function levels. The component PCE models in the PCE-HDMR for the 3D analytical function are depicted in Fig. 3, where circles are sample points and black dots are prediction points. Table 1 compares the performance of the proposed PCE-HDMR and three well-established HDMRs (i.e., RBF-HDMR, SVR-HDMR, and KRG-HDMR) in terms of four performance metrics described in Section 4 and the required number of expensive model evaluations (NOE). Note that the best results, i.e., the largest R^2 value and the smallest RAAE, RMAE, RMSE, and NOE values, are marked in bold. It is observed that the proposed PCE-HDMR outperforms other three HDMRs in terms of all five performance criteria, especially for RAAE, RMAE, and RMSE with 12 to 13 lower orders of magnitude.

4 Numerical results and discussion

4.1 Test suite and setting

In order to comprehensively evaluate the performance of the proposed PCE-HDMR and eliminate the randomness and bias of few test problems, this study establishes a suite of fourteen benchmark functions and five engineering examples consisting of 13 high-dimensional (from 10D to 30D) and 6 low-dimensional (from 2D to 7D) problems. As provided in Table 2, the benchmark functions (Ishigami and Homma 1990; Shan and Wang 2010a; Wang et al. 2011; Cai et al. 2016) have been carefully chosen to demonstrate various aspects of predicted responses such as being highly nonlinear, non-monotonic, and multimodal. For engineering examples given in Table 3, the first one (E1) is the design of a direct cell system using methanol as the fuel to generate electricity via reaction with oxygen in the air (Yang and Xue 2015). The semi-empirical output voltage f_v of a specific fuel cell system is influenced by the current density I (A/cm²), temperature T (K), methanol concentration C_{ME} (M), methanol flow rate F_{ME} (ccm), and air flow rate F_{AIR} (ccm). The second example (E2) is to measure the performance of a piston moving within a cylinder by the time f_c it takes to complete one cycle (Kenett and Zacks 1998). The design variables include the piston weight M (kg), piston surface area S (m²), initial gas volume V_0 (m³), spring coefficient k (N/m), atmospheric pressure P_0 (N/m²), ambient temperature T_a (K), and filling gas temperature T_0 (K). The third example (E3) is to estimate the maximum deflection f_w of a 23-bar truss structure with its upper portion subjected to vertical loads (Blatman and Sudret 2011). The design variables are the Young's moduli E_1 and E_2 (Pa), cross-sectional areas A_1 and A_2 (m²), and applied loads P_1 – P_6 (N). The fourth example (E4) models the tip deflection f_δ of a ten-stepped cantilever beam with a force of $P = 50$ kN in the tip and a material of $E = 2 \times 10^{11}$ Pa and $\sigma_{allow} = 3.5 \times 10^8$ Pa (Cheng et al. 2015). The width b_i (m), height h_i (m), and

Fig. 3 The component PCE models in the PCE-HDMR for the 3D analytical function



length l_i (m) of each step are selected as design variables. This problem is of high complexity as the global optimum is unknown. The last example (E5) is to evaluate the maximum stress σ_{max} (kN/m²) of the main arch structure in a prestressed hydraulic press machinery (Zeng 2009). The design variables are Young's modulus E (Pa), Poisson's ratio μ , inner and outer radii of the main arch R_1 and R_2 (m), column height H

(m), thickness of the arch structure D (m), and operating load P (kN/m²).

Prediction accuracy of the HDMR models can be measured with different kinds of error metrics. To have an exhaustive study on the proposed PCE-HDMR, and also to make a comprehensive comparison with the existing HDMRs, four commonly used performance criteria are selected: coefficient of

Table 1 Performance of PCE-HDMR and three HDMRs for the 3D analytical function

Model	R^2	RAAE	RMAE	RMSE	NOE
RBF-HDMR	9.9999E-01	1.3205E-03	8.5096E-03	8.7807E-04	52.4
SVR-HDMR	9.9998E-01	1.9529E-03	7.9972E-03	1.0775E-03	31.3
KRG-HDMR	9.9988E-01	7.0714E-03	4.2692E-02	4.4642E-03	39.1
PCE-HDMR	1	3.8388E-16	2.0465E-15	2.2203E-16	29

Table 2 Fourteen benchmark functions

No.	Expression	Design space
F1	$f(\mathbf{x}) = 2x_1^2 - 1.05x_1^4 + \frac{x_1^6}{6} - x_1x_2 - x_2^2$	$\mathbf{x} \in [-2, 2]^2$
F2	$f(\mathbf{x}) = \left(x_2 - 1.275\left(\frac{x_1}{\pi}\right)^2 + \frac{5x_1}{\pi} - 6\right)^2 + 10\left(1 - \frac{0.125}{\pi}\right)\cos(x_1) + 10$	$x_1 \in [-5, 0]$ $x_2 \in [10, 15]$
F3	$f(\mathbf{x}) = \sin(x_1) + 7\sin^2(x_2) + 0.1x_1^4\sin(x_3)$	$\mathbf{x} \in [-\pi, \pi]^3$
F4	$f(\mathbf{x}) = x_1^2 + x_2^2 + x_1x_2 - 14x_1 - 16x_2 + (x_3 - 10)^2 + 4(x_4 - 5)^2 + (x_5 - 3)^2 + 2(x_6 - 1)^2 + 5x_7^2 + 7(x_8 - 11)^2 + 2(x_9 - 10)^2 + (x_{10} - 7)^2 + 45$	$\mathbf{x} \in [-10, 11]^{10}$
F5	$f(\mathbf{x}) = \sum_{i=1}^9 \left((x_{i+1}^2 - x_i)^2 + (x_i - 1)^2 \right)$	$\mathbf{x} \in [-3, 3]^{10}$
F6	$f(\mathbf{x}) = \sum_{i=1}^{10} e^{x_i} (c_i + x_i - \ln(\sum_{k=1}^{10} e^{x_k}))$	$\mathbf{x} \in [-5, 5]^{10}$
F7	$f(\mathbf{x}) = \sum_{i=1}^{10} (x_i^2 - 10\cos(2\pi x_i) + 10)$	$\mathbf{x} \in [-1, 1]^{10}$
F8	$f(\mathbf{x}) = \sum_{i=1}^{10} \left[(\ln(x_i - 2))^2 + (\ln(10 - x_i))^2 \right] - \left(\prod_{i=1}^{10} x_i \right)^{0.2}$	$\mathbf{x} \in [2.1, 9.9]^{10}$
F9	$f(\mathbf{x}) = \sum_{i=1}^{10} x_i \left(c_i + \ln \frac{x_i}{x_1 + \dots + x_{10}} \right)$	$\mathbf{x} \in [1e^{-6}, 10]^{10}$
F10	$f(\mathbf{x}) = \sum_{i=1}^{16} \sum_{j=1}^{16} a_{ij} (x_i^2 + x_j + 1) (x_j^2 + x_i + 1)$	$\mathbf{x} \in [0, 5]^{16}$
F11	$f(\mathbf{x}) = (x_1 - 1)^2 + \sum_{i=2}^{16} i(2x_i^2 - x_{i-1})^2$	$\mathbf{x} \in [-5, 5]^{16}$
F12	$f(\mathbf{x}) = \sum_{i=1}^{19} \left((x_{i+1}^2 - x_i)^2 + (x_i - 1)^2 \right)$	$\mathbf{x} \in [-3, 3]^{20}$
F13	$f(\mathbf{x}) = \sum_{i=1}^{20} (x_i^2 - 10\cos(2\pi x_i) + 10)$	$\mathbf{x} \in [-1, 1]^{20}$
F14	$f(\mathbf{x}) = \sum_{i=1}^{29} \left((x_{i+1}^2 - x_i)^2 + (x_i - 1)^2 \right)$	$\mathbf{x} \in [-3, 3]^{30}$

For F6 and F9:

$$\mathbf{c} = -1 \times [6.089, 17.164, 34.054, 5.914, 24.721, 14.986, 24.100, 10.708, 26.662, 22.179]$$

For F10:

$$[a_{ij}]_{\text{rows } 1-8} = \begin{bmatrix} 1 & 0 & 0 & 1 & 0 & 0 & 1 & 1 & 0 & 0 & 0 & 0 & 0 & 0 & 1 \\ 0 & 1 & 1 & 0 & 0 & 0 & 1 & 0 & 0 & 1 & 0 & 0 & 0 & 0 & 0 \\ 0 & 0 & 1 & 0 & 0 & 0 & 1 & 0 & 1 & 1 & 0 & 0 & 0 & 1 & 0 \\ 0 & 0 & 0 & 1 & 0 & 0 & 1 & 0 & 0 & 0 & 1 & 0 & 0 & 0 & 1 \\ 0 & 0 & 0 & 0 & 1 & 1 & 0 & 0 & 0 & 1 & 0 & 1 & 0 & 0 & 1 \\ 0 & 0 & 0 & 0 & 0 & 1 & 0 & 1 & 0 & 0 & 0 & 0 & 0 & 1 & 0 \\ 0 & 0 & 0 & 0 & 0 & 0 & 1 & 0 & 0 & 0 & 1 & 0 & 1 & 0 & 0 \\ 0 & 0 & 0 & 0 & 0 & 0 & 0 & 1 & 0 & 1 & 0 & 0 & 0 & 1 & 0 \end{bmatrix}$$

$$[a_{ij}]_{\text{rows } 9-16} = \begin{bmatrix} 0 & 0 & 0 & 0 & 0 & 0 & 0 & 0 & 1 & 0 & 0 & 1 & 0 & 0 & 0 & 1 \\ 0 & 0 & 0 & 0 & 0 & 0 & 0 & 0 & 0 & 1 & 0 & 0 & 0 & 1 & 0 & 0 \\ 0 & 0 & 0 & 0 & 0 & 0 & 0 & 0 & 0 & 0 & 1 & 0 & 1 & 0 & 0 & 0 \\ 0 & 0 & 0 & 0 & 0 & 0 & 0 & 0 & 0 & 0 & 0 & 1 & 0 & 1 & 0 & 0 \\ 0 & 0 & 0 & 0 & 0 & 0 & 0 & 0 & 0 & 0 & 0 & 0 & 1 & 1 & 0 & 0 \\ 0 & 0 & 0 & 0 & 0 & 0 & 0 & 0 & 0 & 0 & 0 & 0 & 0 & 1 & 0 & 0 \\ 0 & 0 & 0 & 0 & 0 & 0 & 0 & 0 & 0 & 0 & 0 & 0 & 0 & 0 & 1 & 0 \\ 0 & 0 & 0 & 0 & 0 & 0 & 0 & 0 & 0 & 0 & 0 & 0 & 0 & 0 & 0 & 1 \end{bmatrix}$$

determination (R^2), relative average absolute error (RAAE), relative maximum absolute error (RMAE), and root mean square error (RMSE). They are formulated as follows:

$$R^2 = 1 - \frac{\sum_{i=1}^{nt} [f(\mathbf{x}_i) - \hat{f}(\mathbf{x}_i)]^2}{\sum_{i=1}^{nt} [f(\mathbf{x}_i) - \bar{f}]^2} \quad (36)$$

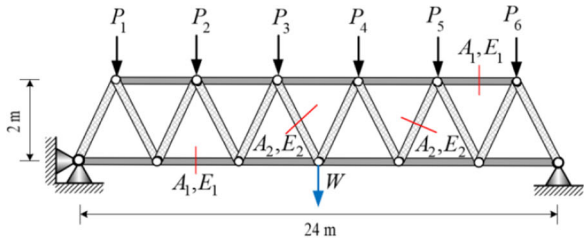
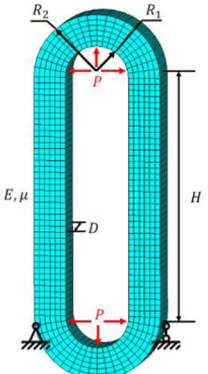
$$RAAE = \frac{\sum_{i=1}^{nt} |f(\mathbf{x}_i) - \hat{f}(\mathbf{x}_i)|}{nt \times std} \quad (37)$$

$$RMAE = \frac{\max_{1 \leq i \leq nt} |f(\mathbf{x}_i) - \hat{f}(\mathbf{x}_i)|}{std} \quad (38)$$

$$RMSE = \sqrt{\frac{\sum_{i=1}^{nt} [f(\mathbf{x}_i) - \hat{f}(\mathbf{x}_i)]^2}{nt}} \quad (39)$$

where nt is the number of test points, \mathbf{x}_i is one of the nt test points, \bar{f} is the average response over the nt points, and std stands for standard deviation of the function responses at nt test points. It is apparent that R^2 , RAAE, and RMSE provide global error measurements over the entire design domain,

Table 3 Five engineering examples

No.	Expression	Design space
E1	$f_V = 1.21 - 3.7534 \times 10^{-5}T - 3.1534 \times 10^{-4}T \ln C_{ME}$ $+ 6.62 \times 10^{-5}T \ln F_{AIR} - 0.7499 - 6.9897e^{\left(\frac{916.91}{T} - 4.6392\right)I}$ $- [1.2658 \times 10^5 I^3 + 46196 I^2 - 4281 I - 0.4029 T - 18.8094 C_{ME}^2$ $+ 18.8094 C_{ME} + 10.496] \times [\ln I - 3.9056 + 2.9582 \times 10^{-4}(\ln C_{ME}$ $+ \ln(1 - \frac{1}{5.3466 \times 10^7 e^{(-5182.4/T)} C_{ME}^2} I))] - [-1.2687 \times 10^5 I^3 -$ $46221 I^2 + 4283.6 I + 0.4033 T + 18.818 C_{ME}^2 - 18.818 C_{ME} -$ $10.572] \times [\ln I - 3.8959 - 8.2402 \times 10^{-4} \ln F_{AIR}] + 31.583 I^2 \ln F_{ME}$	$I \in [0.0003, 0.08]$ $T \in [298, 343]$ $C_{ME} \in [0.25, 2]$ $F_{ME} \in [3.5, 5.5]$ $F_{AIR} \in [81.2, 140.8]$
E2	$f_c = 2\pi \sqrt{\frac{M}{k + S^2 \frac{P_0 V_0 T_a}{T_0 V^2}}}, \text{ where}$ $V = \frac{S}{2k} \left(\sqrt{A^2 + 4k \frac{P_0 V_0}{T_0} T_a} - A \right), A = P_0 S + 19.62 M - \frac{k V_0}{S}$	$M \in [30, 60]$ $S \in [0.005, 0.020]$ $V_0 \in [0.002, 0.010]$ $k \in [1000, 5000]$ $P_0 \in [90000, 110000]$ $T_a \in [290, 296]$ $T_0 \in [340, 360]$
E3		E_1, E_2 $\in [1.89, 2.31] \times 10^{11}$ $A_1 \in [1.8, 2.2] \times 10^{-3}$ $A_2 \in [0.9, 1.1] \times 10^{-3}$ P_1, \dots, P_6 $\in [4.25, 5.75] \times 10^4$
E4	$f_\delta = \int_0^{l_d} \frac{P x_d^2}{EI_d} dx_d + \int_0^{l_{d-1}} \frac{P(x_{d-1} + l_d)^2}{EI_{d-1}} dx_{d-1} + \dots$ $+ \int_0^{l_1} \frac{P(x_1 + l_2 + l_3 + \dots + l_d)^2}{EI_1} dx_1$ $= \frac{P}{3E} \sum_{i=1}^d \left[\frac{12}{b_i h_i^3} \left(\left(\sum_{j=i}^d l_j \right)^3 - \left(\sum_{j=i+1}^d l_j \right)^3 \right) \right]$	$b_i \in [0.01, 0.05]$ $h_i \in [0.3, 0.65]$ $l_i \in [0.5, 1]$ where $1 \leq i \leq 10$
E5		$E \in [1.68, 2.52] \times 10^{11}$ $\mu \in [0.24, 0.36]$ $R_1 \in [2.0, 2.5]$ $R_2 \in [4.25, 4.75]$ $H \in [16, 18]$ $D \in [3.15, 3.65]$ $P \in [2.09, 3.14] \times 10^4$

while RMAE is indicative of local deviations between the predictions and true responses. R^2 ranges from 0 to 1. The larger value the R^2 has, the more accurate the HDMR model is. For metrics RAAE, RMAE, and RMSE, when their values are smaller, the metamodel is more accurate. These performance criteria are calculated using $nt = 5000$ randomly selected test points, and the process is repeated for ten times to obtain robust results with the mean values.

4.2 Results and discussion

4.2.1 Comparison with other HDMRs

In the numerical experiments, a detailed comparison between the proposed PCE-HDMR and other well-established HDMRs including RBF-HDMR, SVR-HDMR, and KRG-HDMR has been carried out. DIRECT sampling method is adopted for all four HDMRs. Table 4 provides the modeling results of the four HDMRs for the fourteen benchmark functions and five engineering examples. The best results are marked in bold. The data shows the Cut-HDMR structure is effective in approximating various problems of both high and low dimensions, except that RBF-HDMR gives undesirable results for functions F7 (10D) and F13 (20D). From the overall comparison, it is observed that the proposed PCE-HDMR has the best accuracy in terms of R^2 , RAAE, RMAE, and RMSE for 16 out of 19 test problems (except for the second best RMAE values of F9, E3, and E4 and RAAE value of E4 and the comparable RMAE value of E2) and best efficiency in terms of NOE for 16 out of 19 test problems. On the other hand, in terms of R^2 , RAAE, RMAE, and RMSE, RBF-HDMR is superior to SVR-HDMR and KRG-HDMR for test problems F1, F2, F4, F5, F6, F10, F11, F12, F14, and E3, while SVR-HDMR outperforms RBF-HDMR and KRG-HDMR for F3, F13, and E1, and KRG-HDMR is more desirable than RBF-HDMR and SVR-HDMR for F7 and F8. However, RBF-HDMR is less efficient than both SVR-HDMR and KRG-HDMR in terms of NOE for 17 out of 19 test problems. As described in Section 1, this demonstrates the prediction uncertainty usually encountered by the existing stand-alone Cut-HDMRs such as RBF-HDMR, SVR-HDMR, and KRG-HDMR. In summary, as a novel stand-alone Cut-HDMR, the PCE-HDMR is robust, accurate, and efficient in modeling a variety of problems including engineering examples compared with other stand-alone Cut-HDMRs, especially when it is very difficult (if not impossible) to know a priori which HDMR model is most desirable for an unknown problem.

It is also noted from Table 4 that for the test problems in purely polynomial form, e.g., F1 (2D, six-order polynomial), F4 (10D, second-order polynomial), F5 (10D, four-order polynomial), F11 (16D, four-order polynomial), F12 (20D, four-order polynomial), and F14 (30D, four-order

polynomial), the PCE-HDMR can produce super accurate results with the R^2 value of exact 1, RAAE value of 10^{-16} – 10^{-15} , RMAE value of 10^{-15} – 10^{-14} , and RMSE value of 10^{-14} – 10^{-11} , no matter whether the problem dimension and polynomial order are high or low. The values of RAAE, RMAE, and RMSE by the PCE-HDMR are 12 to 14 orders of magnitude lower than those by RBF-HDMR, SVR-HDMR, and KRG-HDMR. For the non-polynomial functions such as F2, F3, and F13, the results of RAAE, RMAE, and RMSE by the PCE-HDMR are still several orders (ranging from 1 to 6) of magnitude more accurate than those by the other three HDMRs, and for complex engineering examples such as E1, E3, and E4, they are generally much lower than those by other benchmark HDMRs. The above superiority of the PCE-HDMR is attributed to the high reproducibility and capability of the PCE in the form of expanded multivariate orthonormal polynomials in constructing the component functions of Cut-HDMR. Overall, the proposed PCE-HDMR is more capable and versatile than the benchmark HDMRs in modeling problems of both functional form and engineering practice.

The effect of problem dimensionality on the accuracy and efficiency of the proposed PCE-HDMR and other three benchmark HDMRs is investigated. Functions F5, F12, and F14 in Table 2 have the same expression but different dimensions of 10, 20, and 30, respectively. As the dimension increases, it can be seen from Table 4 that for the three benchmark HDMRs, the accuracy in terms of R^2 , RAAE, RMAE, and RMSE and efficiency in terms of NOE generally decrease. However, as the dimension increases from 10 to 30, the R^2 value remains exactly 1 for the PCE-HDMR, which indicates its robustness and reproducibility in modeling high-dimensional problems. Also, functions F7 and F13 have the same expression but different dimensions of 10 and 20, respectively. It is worthy to note that KRG-HDMR has the best accuracy for F7, while PCE-HDMR is the second best. When the dimension increases to 20 (i.e., F13), PCE-HDMR outperforms KRG-HDMR and two other benchmark HDMRs in terms of all five performance criteria. This indicates that the superiority of the PCE-HDMR over other benchmark HDMRs becomes more significant for problems with higher dimensions.

To have a general perspective of the overall performances, Table 5 compares the mean values and standard deviations of all the error metrics (R^2 , RAAE, RMAE, and RMSE) for the proposed PCE-HDMR and other three HDMRs across all nineteen test problems. The best results are marked in bold. It is observed that the proposed PCE-HDMR obtains the best global performance in terms of both accuracy and robustness based on all four error metrics (except that the robustness of PCE-HDMR in terms of RMSE is the second best and very close to that of RBF-HDMR). Among the three benchmark algorithms, KRG-HDMR has the best accuracy and

Table 4 Comparison of PCE-HDMR and other HDMRs for the fourteen benchmark functions and five engineering examples

f	Model	R^2	RAAE	RMAE	RMSE	NOE
F1	RBF-HDMR	1.0000	0.0005	0.0037	0.0014	47.2
	SVR-HDMR	0.9955	0.0292	0.0587	0.0613	26
	KRG-HDMR	0.9999	0.0050	0.0350	0.0151	33.8
	PCE-HDMR	1	9.0917E-15	3.5186E-14	2.1604E-14	22
F2	RBF-HDMR	1.0000	0.0007	0.0047	0.0403	28
	SVR-HDMR	0.9992	0.0159	0.0328	0.6326	19.1
	KRG-HDMR	1.0000	0.0033	0.0200	0.1825	20.8
	PCE-HDMR	1.0000	9.0045E-08	7.2449E-07	6.0352E-06	20
F3	RBF-HDMR	0.9945	0.0575	0.2735	0.2663	126
	SVR-HDMR	0.9991	0.0142	0.1477	0.0878	91.2
	KRG-HDMR	0.9912	0.0329	0.5387	0.2634	78
	PCE-HDMR	1.0000	0.0025	0.0294	0.0171	63
F4	RBF-HDMR	1.0000	0.0001	0.0011	0.2322	125.5
	SVR-HDMR	1.0000	0.0010	0.0030	1.2590	109.1
	KRG-HDMR	1.0000	0.0005	0.0029	0.8045	124.5
	PCE-HDMR	1	3.2488E-16	2.0509E-15	4.5058E-13	100
F5	RBF-HDMR	9.9999E-01	0.0017	0.0138	0.2351	317.8
	SVR-HDMR	0.9589	0.1491	0.5897	17.5810	203.4
	KRG-HDMR	0.9993	0.0176	0.1103	2.3050	258.4
	PCE-HDMR	1	5.1717E-16	3.6499E-15	6.5406E-14	159
F6	RBF-HDMR	0.9967	0.0352	0.5253	1.1758E+02	1116.1
	SVR-HDMR	0.9906	0.0636	0.6935	1.9933E+02	724.6
	KRG-HDMR	0.9867	0.0769	0.7528	2.3803E+02	700.2
	PCE-HDMR	0.9950	0.0507	0.5137	1.4527E+02	366.6
F7	RBF-HDMR	0.5872	0.5653	1.7221	14.2167	226
	SVR-HDMR	1.0000	0.0034	0.0200	0.1014	181.1
	KRG-HDMR	1.0000	0.0000	0.0000	0.0001	186
	PCE-HDMR	1.0000	0.0032	0.0180	0.0915	176
F8	RBF-HDMR	0.9737	0.1242	0.7038	1.4650	774.9
	SVR-HDMR	0.9709	0.1295	0.7369	1.5357	666.1
	KRG-HDMR	0.9787	0.1108	0.6835	1.3096	571.2
	PCE-HDMR	0.9867	0.0872	0.5289	1.0298	643.4
F9	RBF-HDMR	1.0000	0.0021	0.0207	0.5518	264.2
	SVR-HDMR	1.0000	0.0034	0.0238	0.9048	306
	KRG-HDMR	1.0000	0.0024	0.0170	0.6301	266
	PCE-HDMR	1.0000	0.0014	0.0172	0.4067	276
F10	RBF-HDMR	1.0000	0.0035	0.0206	12.4037	674.3
	SVR-HDMR	0.9988	0.0268	0.1111	86.0848	430.3
	KRG-HDMR	0.9996	0.0146	0.0843	49.8638	439.7
	PCE-HDMR	1	2.5176E-09	1.1454E-08	8.3332E-06	368
F11	RBF-HDMR	1.0000	0.0009	0.0066	33.5990	611.2
	SVR-HDMR	0.9908	0.0742	0.3076	2.4441E+03	398.3
	KRG-HDMR	0.9997	0.0119	0.0641	4.1724E+02	437.7
	PCE-HDMR	1	6.2265E-16	4.1797E-15	2.2146E-11	307
F12	RBF-HDMR	9.9993E-01	0.0049	0.0350	0.9656	722
	SVR-HDMR	0.9454	0.1838	0.8379	31.3501	488.1
	KRG-HDMR	0.9990	0.0234	0.1234	4.1304	609.9
	PCE-HDMR	1	8.1306E-16	5.7474E-15	1.4856E-13	424

Table 4 (continued)

f	Model	R^2	RAAE	RMAE	RMSE	NOE
F13	RBF-HDMR	2.8925E-01	0.7785	1.9465	26.3810	551
	SVR-HDMR	9.9998E-01	0.0035	0.0178	0.1411	456
	KRG-HDMR	9.9558E-01	0.0570	0.2213	2.0737	411
	PCE-HDMR	9.9999E-01	0.0022	0.0113	0.0883	351
F14	RBF-HDMR	9.9991E-01	0.0058	0.0400	1.4202	1255.1
	SVR-HDMR	9.5267E-01	0.1734	0.7657	36.6833	878.7
	KRG-HDMR	9.9831E-01	0.0322	0.1685	6.8943	1048.9
	PCE-HDMR	1	1.1841E-15	7.7783E-15	2.6148E-13	789
E1	RBF-HDMR	0.9324	0.1425	1.2719	0.0441	315.1
	SVR-HDMR	0.9972	0.0322	0.3070	0.0103	167.7
	KRG-HDMR	0.9851	0.0605	0.6037	0.0194	174.6
	PCE-HDMR	0.9978	0.0280	0.2734	0.0091	153.6
E2	RBF-HDMR	0.9815	0.0794	1.5096	0.0188	180.6
	SVR-HDMR	0.9809	0.0766	1.4939	0.0192	174.3
	KRG-HDMR	0.9813	0.0734	1.5274	0.0191	163.2
	PCE-HDMR	0.9821	0.0725	1.5292	0.0187	157.5
E3	RBF-HDMR	9.9999E-01	0.0017	0.0114	1.4186E-05	209.8
	SVR-HDMR	9.9986E-01	0.0050	0.0230	4.0747E-05	219.2
	KRG-HDMR	9.9995E-01	0.0051	0.0232	4.0567E-05	187.9
	PCE-HDMR	1.0000	0.0011	0.0115	1.1426E-05	165.4
E4	RBF-HDMR	9.9305E-01	0.0375	1.3030	186.9312	1088
	SVR-HDMR	9.9328E-01	0.0461	1.2816	180.2053	854.7
	KRG-HDMR	9.9313E-01	0.0447	1.2049	181.9374	835.9
	PCE-HDMR	9.9333E-01	0.0437	1.2368	177.7583	805.7
E5	RBF-HDMR	0.9999	0.0051	0.0516	58.8086	120.6
	SVR-HDMR	0.9999	0.0061	0.0450	65.5325	112.6
	KRG-HDMR	0.9999	0.0070	0.0481	73.5540	105
	PCE-HDMR	0.9999	0.0059	0.0481	63.5316	98.8

robustness in terms of R^2 , RAAE, and RMAE, followed by SVR-HDMR and RBF-HDMR. Nevertheless, RBF-HDMR outperforms in terms of RMSE, followed by KRG-HDMR and SVR-HDMR. This shows again the prediction uncertainty for the existing RBF-HDMR, SVR-HDMR, and KRG-HDMR. Boxplots of the four error metrics for the PCE-HDMR and benchmark algorithms are depicted in Fig. 4, which validates the findings from Table 5. It is shown that the PCE-HDMR achieves the best medians (highest for R^2 and lowest for RAAE, RMAE, and RMSE) and shortest interquartile range among all the algorithms.

To further analyze the error values, formal significance tests are conducted for more rigorous comparisons. As the boxplots in Fig. 4 show that the error values are highly skewed and do not satisfy the requirements of the classical t -test (Li et al. 2010; Gibbons and Chakraborti 2014), the assumption-free Wilcoxon signed-rank test (significance level of 0.05 with two tails) is employed to test the matched HDMR pairs. The

p values of Wilcoxon signed-rank tests are presented in the upper triangle of Table 6. It can be found that PCE-HDMR significantly outperforms RBF-HDMR, SVR-HDMR, and KRG-HDMR under all error metrics with the p values much smaller than 0.05. It is also seen that regarding the error metrics R^2 , RAAE, and RMAE, there are no statistically significant differences in the paired comparisons among RBF-HDMR, SVR-HDMR, and KRG-HDMR. These findings demonstrate again that PCE-HDMR is the most accurate algorithm among the four HDMR metamodels.

4.2.2 Impact of the PCE degree

To explore the effect of the PCE degrees p_1 and p_2 respectively adopted in the 1D and 2D PCE models on the accuracy and efficiency of the proposed PCE-HDMR, a non-polynomial function F6 (10D) is selected as a representative for further study. Table 7 and Table 8 give the results of five performance

Table 5 Comparison of the average accuracy and robustness for the PCE-HDMR and other HDMRs across all test problems

Model	Error metrics							
	R^2		RAAE		RMAE		RMSE	
	Mean	Std	Mean	Std	Mean	Std	Mean	Std
RBF-HDMR	0.980	0.043	0.060	0.101	0.409	0.539	22.842	49.332
SVR-HDMR	0.988	0.018	0.055	0.061	0.395	0.460	161.346	556.044
KRG-HDMR	0.995	0.007	0.030	0.032	0.328	0.444	51.540	110.892
PCE-HDMR	0.998	0.005	0.016	0.027	0.222	0.444	20.433	52.071

criteria varying with the PCE degrees p_1 and p_2 , respectively. For the convenience of comparison, these results are also depicted in Figs. 5, 6, 7 and 8.

It is observed that compared with the error metrics of RMAE and RMSE, the variations of R^2 and RAAE are almost negligible as the PCE degrees of p_1 and p_2 change from 6 to 14

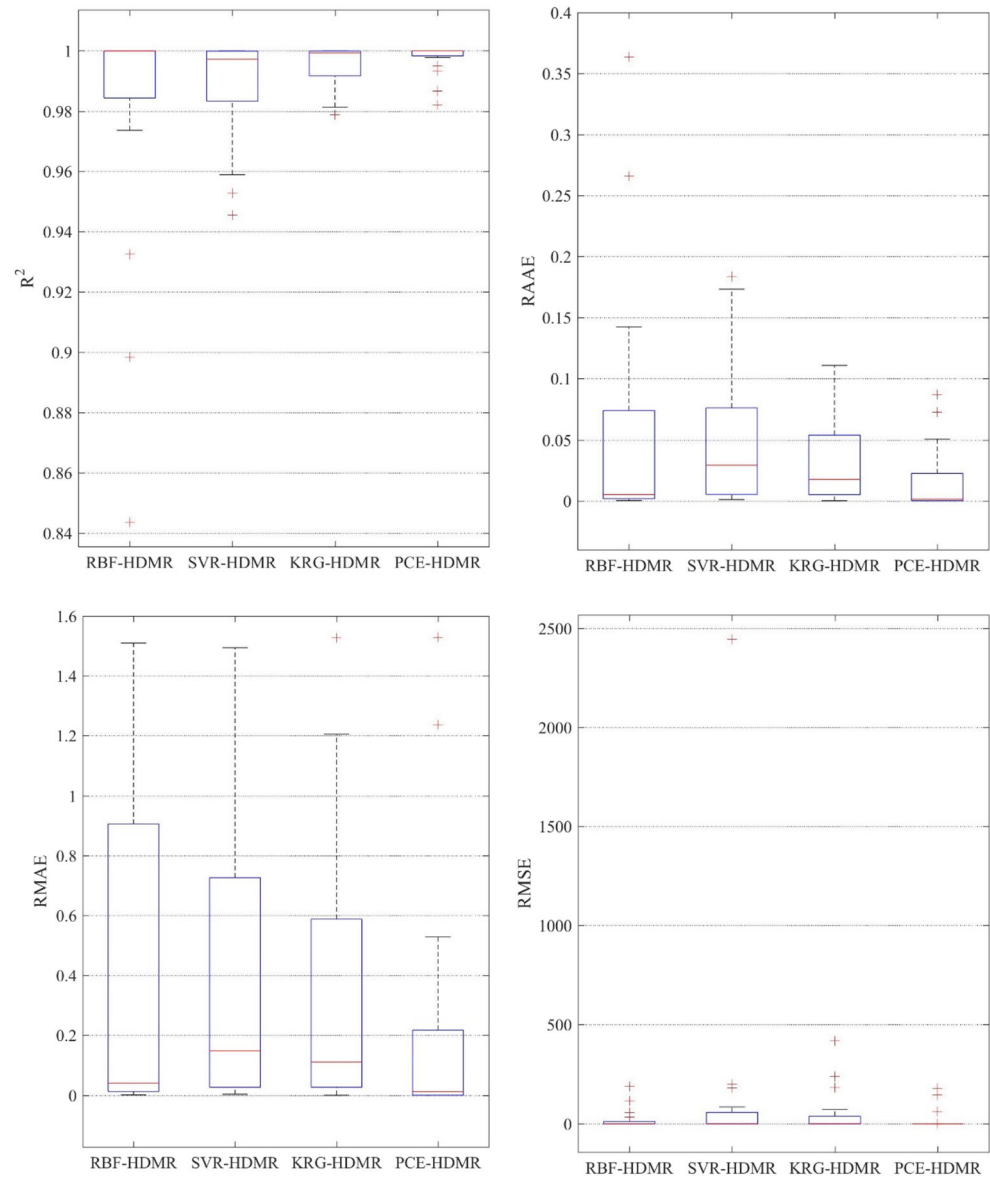
Fig. 4 Boxplots of four error metrics: R^2 , RAAE, RMAE, and RMSE

Table 6 p values of Wilcoxon signed-rank tests

Error metrics	Model	RBF-HDMR	SVR-HDMR	KRG-HDMR	PCE-HDMR
R^2	RBF-HDMR	—	0.314	0.421	0.003
	SVR-HDMR	—	—	0.159	1.318E-04
	KRG-HDMR	—	—	—	2.137E-04
RAAE	RBF-HDMR	—	0.260	0.717	0.011
	SVR-HDMR	—	—	0.107	1.318E-04
	KRG-HDMR	—	—	—	3.416E-04
RMAE	RBF-HDMR	—	0.520	0.520	0.001
	SVR-HDMR	—	—	0.295	0.001
	KRG-HDMR	—	—	—	0.003
RMSE	RBF-HDMR	—	0.044	0.126	0.010
	SVR-HDMR	—	—	0.198	1.318E-04
	KRG-HDMR	—	—	—	2.926E-04

Table 7 Effect of the PCE degree p_1 on the performance criteria for function F6 with $p_2 = 15$

p_1	R^2	RAAE	RMAE	RMSE	NOE
6	0.9946	0.0530	0.5215	151.2133	407.2
7	0.9948	0.0511	0.5271	149.1394	370.4
8	0.9947	0.0511	0.5271	150.2379	369.4
9	0.9947	0.0515	0.5259	149.4615	366.9
10	0.9949	0.0509	0.5003	147.0999	362.9
11	0.9949	0.0510	0.5126	146.7669	368.6
12	0.9946	0.0524	0.4814	151.4693	374.9
13	0.9951	0.0493	0.5340	143.9815	368
14	0.9950	0.0496	0.5035	145.6823	368.2

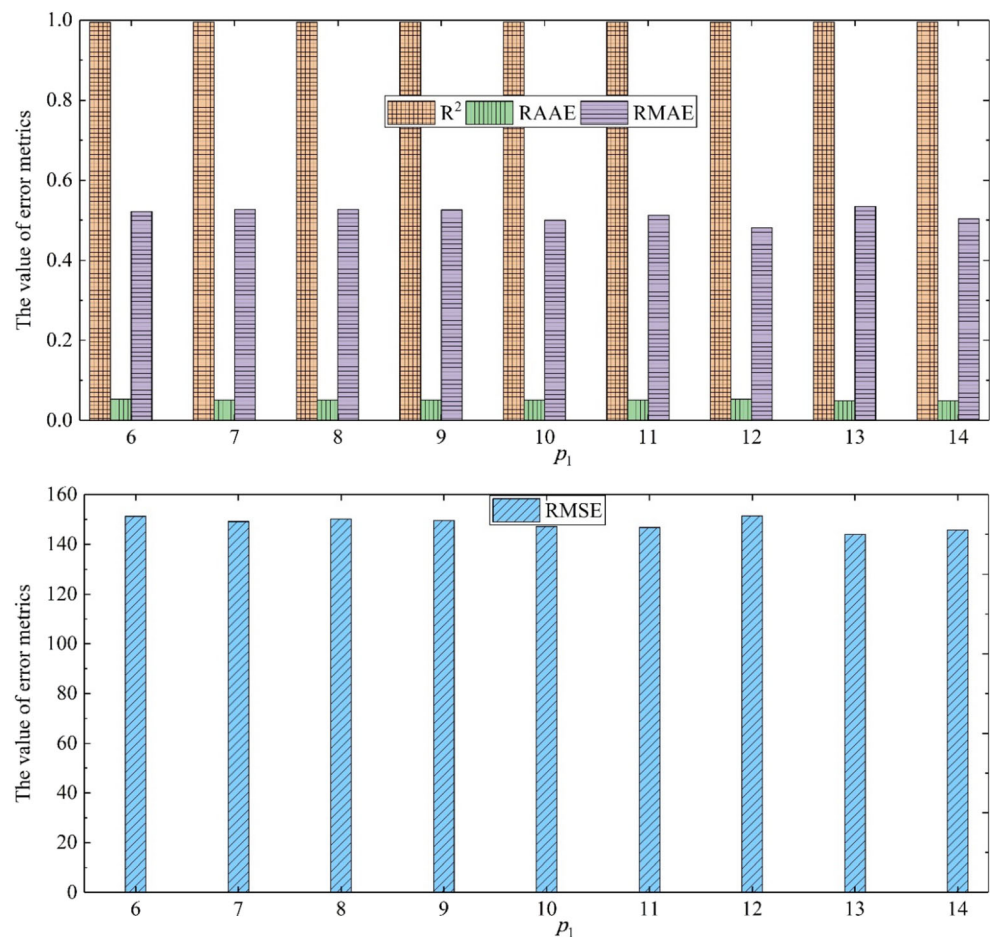
and from 11 to 19, respectively. On the other hand, when the PCE degree p_1 is bigger than 10 (p_2 is fixed at 15), the values of RMAE and RMSE are generally lower than those with p_1 less than 10 (except for the RMAE value with $p_1 = 13$ and the RMSE value with $p_1 = 12$). This indicates that a larger value of p_1 , i.e., $p_1 \geq 10$, is preferred in the PCE-HDMR. In terms of

efficiency, the NOE reaches its minimum value when $p_1 = 10$, as shown in Fig. 7. To this end, a value of $p_1 = 10$ is recommended for the PCE-HDMR. Similarly, in consideration of both accuracy and efficiency when p_2 varies from 11 to 19 with p_1 fixed at 10, a value of $p_2 = 15$ is suggested. Therefore, the values of $p_1 = 10$ and $p_2 = 15$ are recommended for the

Table 8 Effect of the PCE degree p_2 on the performance criteria for function F6 with $p_1 = 10$

p_2	R^2	RAAE	RMAE	RMSE	NOE
11	0.9952	0.0484	0.5408	141.9338	366.2
12	0.9945	0.0519	0.5271	153.9544	367.2
13	0.9948	0.0509	0.5102	148.0988	367.5
14	0.9951	0.0498	0.4821	143.7930	365.3
15	0.9949	0.0509	0.5003	147.0999	362.9
16	0.9947	0.0512	0.5618	150.9600	365.9
17	0.9949	0.0501	0.4807	146.0904	368.2
18	0.9948	0.0506	0.5070	149.3687	367
19	0.9949	0.0504	0.4976	147.1583	369.4

Fig. 5 Effect of the PCE degree p_1 in the PCE-HDMR on the values of R^2 , RAAE, RMAE, and RMSE for function F6 with $p_2 = 15$



proposed PCE-HDMR and have been used for the fourteen benchmark functions and five engineering examples in this study.

4.2.3 Running time

To illustrate the modeling efficiency, Table 9 provides the running times of the PCE-HDMR and three benchmark HDMRs for all the nineteen cases. All the numerical experiments are performed in a MATLAB environment with an AMD 3.60 GHz CPU. It is found that the RBF-HDMR has the best efficiency in terms of the model running time, followed by KRG-HDMR, PCE-HDMR, and SVR-HDMR. However, as described in Subsection 4.2.1, RBF-HDMR requires the largest number of NOE (i.e., samples) for 17 out of 19 test problems among all four algorithms. The running time of PCE-HDMR mainly comes from the process of constructing the component functions of Cut-HDMR by using the PCE and solving the corresponding PC coefficients.

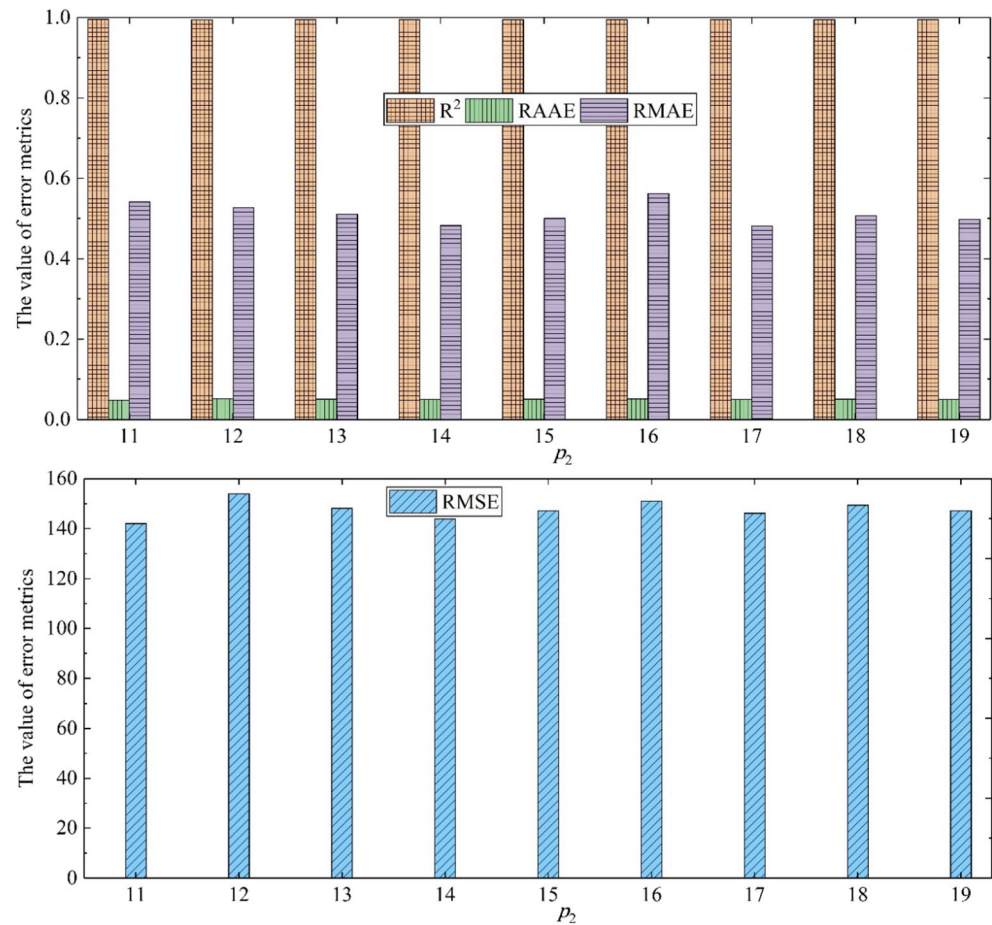
It is worth noting that the PCE-HDMR model is proposed for expensive simulation-based problems, in which a typical simulation may need several hours or even a few days (Gorissen et al. 2007). Therefore, in practice, the running time

of PCE-HDMR is negligible compared to the time spent on simulations. Although the running time of PCE-HDMR itself is generally larger than those of the RBF-HDMR and KRG-HDMR, a great saving in the time spent on simulations has been made by the proposed PCE-HDMR. As shown in Table 4, for example, the RBF-HDMR requires 1255 samples (simulations) to achieve the model accuracy of $R^2 = 9.9991\text{E} - 01$, RAAE = 0.0058, RMAE = 0.0400, and RMSE = 1.4202 for the F14 (30D) case, whereas a much higher model accuracy of $R^2 = 1$, RAAE = $1.1841\text{E} - 15$, RMAE = $7.7783\text{E} - 15$, and RMSE = $2.6148\text{E} - 13$ is achieved by the PCE-HDMR with only 789 samples.

5 Conclusions

This article proposes a novel metamodeling approach, namely an adaptive PCE-HDMR, for high-dimensional problems. In the PCE-HDMR, the PCE metamodel in the form of multivariate orthonormal polynomials is employed for constructing the component functions of the hierarchical Cut-HDMR. The DIRECT sampling method is incorporated into the PCE-HDMR to adaptively refine the model in a robust and efficient

Fig. 6 Effect of the PCE degree p_2 in the PCE-HDMR on the values of R^2 , RAAE, RMAE, and RMSE for function F6 with $p_1 = 10$



way. The performance of the proposed PCE-HDMR is examined by fourteen benchmark functions and five engineering examples consisting of thirteen high-dimensional and six low-dimensional problems and compared with three well-established HDMRs. The effects of functional form, problem dimensionality, and PCE degree on the accuracy and efficiency of the PCE-HDMR are also investigated. From the

extensive numerical results, some concluding remarks can be drawn as follows:

- Compared with the well-established stand-alone Cut-HDMRs, e.g., RBF-HDMR, SVR-HDMR, and KRG-HDMR, the proposed PCE-HDMR as a novel stand-alone Cut-HDMR provides more accurate and robust

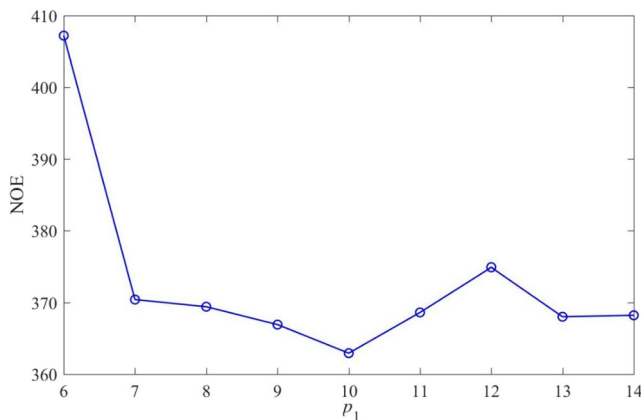


Fig. 7 Effect of the PCE degree p_1 in the PCE-HDMR on the NOE for function F6 with $p_2 = 15$

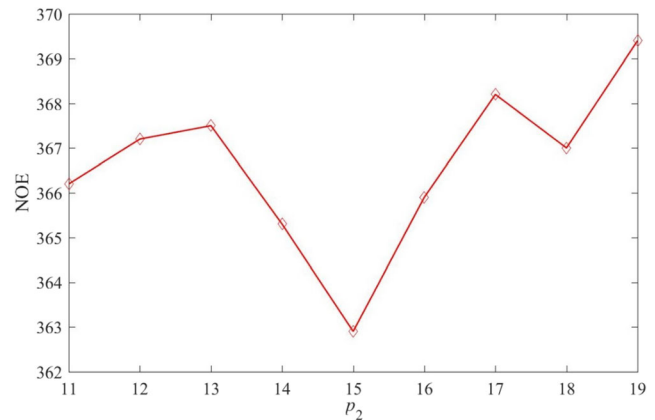


Fig. 8 Effect of the PCE degree p_2 in the PCE-HDMR on the NOE for function F6 with $p_1 = 10$

Table 9 The running times (s) of the PCE-HDMR and other benchmark HDMRs for the fourteen benchmark functions and five engineering examples

Model	F1	F2	F3	F4	F5	F6	F7	F8	F9	F10
RBF-HDMR	2.4	2.4	3.9	12.6	13.2	16.6	13.1	20.0	14.9	23.8
SVR-HDMR	9.0	9.2	24.3	26.2	54.2	215.1	40.6	194.8	106.6	116.6
KRG-HDMR	4.8	2.5	7.7	25.5	26.3	30.7	25.9	35.2	30.8	52.7
PCE-HDMR	5.6	3.3	8.4	25.4	32.9	65.0	25.1	69.6	66.8	72.8
Model	F11	F12	F13	F14	E1	E2	E3	E4	E5	
RBF-HDMR	22.1	27.3	26.7	38.5	7.7	9.3	13.1	37.0	223.5	
SVR-HDMR	95.7	109.9	80.3	149.2	47.2	57.7	70.5	133.4	254.2	
KRG-HDMR	44.3	55.3	53.2	76.0	11.9	16.3	25.9	74.4	230.8	
PCE-HDMR	54.2	67.4	50.8	93.6	16.8	31.1	42.4	87.9	247.5	

predictions in terms of both global (R^2 , RAAE, and RMSE) and local (RMAE) error measurements and needs far fewer number of expensive model evaluations/simulations for a vast majority of test problems including engineering examples.

- Due to the capability and reproducibility of the PCE, the superiority of the PCE-HDMR over other benchmark HDMRs is more significant for functions of more polynomial-like forms, problems with higher dimensions, and PCE degrees with relatively larger values ($p_1 = 10$ and $p_2 = 15$ are recommended).
- Although PCE-HDMR spends more running time than RBF-HDMR and KRG-HDMR for most test problems in this study, it has made a large portion of time-saving on the expensive simulations, compared to which the extra running time of PCE-HDMR is negligible.

In this article, the DIRECT sampling method is adopted to adaptively refine the PCE-HDMR model. It is worth noting that the proposed algorithm can also use other adaptive sampling algorithms such as the maximin sampling approach (Johnson et al. 1990) and CV-Voronoi sampling approach (Xu et al. 2014). In addition, besides the adopted Legendre polynomials, other types of univariate orthogonal polynomials (Xiu and Karniadakis 2002) can be used for constructing the polynomial chaos in the PCE-HDMR.

At current stage, a second-order HDMR expansion is adopted for the proposed PCE-HDMR. In this regard, the main disadvantage of the method is that, for an underlying problem with highly correlated variables, the proposed algorithm may not work well. Further improvements and techniques are needed to extend beyond the second order while keeping the computational cost affordable. Moreover, new development is demanded to incorporate existing samples and/or noisy expansive model into the present PCE-HDMR for engineering practice.

Supplementary Information The online version contains supplementary material available at <https://doi.org/10.1007/s00158-021-02866-7>.

Funding This work was supported by the National Natural Science Foundation of China (Grant Nos. 11872190, 51805221), Six Talent Peaks Project in Jiangsu Province (Grant No. 2017-KTHY-010), and Research Start-up Foundation for Jinshan Distinguished Professor at Jiangsu University (Grant No. 4111480003).

Compliance with ethical standards

Conflict of interest The authors declare that they have no conflict of interest.

Replication of results The original codes for the illustrative example in Section 3.4 and fourteen benchmark functions and five engineering examples in Section 4 are available in the supplementary materials, i.e., IllustrativeExample.m, F1.m ~ F15.m, and E1.m ~ E5.m.

References

- Baptista R, Stolbunov V, Nair PB (2019) Some greedy algorithms for sparse polynomial chaos expansions. *J Comput Phys* 387:303–325
- Blatman G, Sudret B (2011) Adaptive sparse polynomial chaos expansion based on least angle regression. *J Comput Phys* 230:2345–2367
- Cai XW, Qiu HB, Gao L, Yang P, Shao XY (2016) An enhanced RBF-HDMR integrated with an adaptive sampling method for approximating high dimensional problems in engineering design. *Struct Multidiscip Optim* 53(6):1209–1229
- Chen SS, Donoho DL, Saunders MA (1998) Atomic decomposition by basis pursuit. *SIAM J Sci Comput* 20(1):33–61
- Chen LM, Li EY, Wang H (2016) Time-based reflow soldering optimization by using adaptive Kriging-HDMR method. *Soldering Surf Mount Technol* 28(2):101–113
- Chen LM, Wang H, Ye F, Hu W (2019) Comparative study of HDMRs and other popular metamodeling techniques for high dimensional problems. *Struct Multidiscip Optim* 59(1):21–42
- Cheng GH, Younis A, Hajikolaie KH, Wang GG (2015) Trust region based mode pursuing sampling method for global optimization of high dimensional design problems. *J Mech Des* 137(2):021407
- Cheng K, Lu ZZ, Ling CY, Zhou ST (2020) Surrogate-assisted global sensitivity analysis: an overview. *Struct Multidiscip Optim* 61(3):1187–1213
- Chowdhury R, Rao BN (2009) Hybrid high dimensional model representation for reliability analysis. *Comput Methods Appl Mech Eng* 198(5–8):753–765

- Clarke SM, Griebisch JH, Simpson TW (2005) Analysis of support vector regression for approximation of complex engineering analyses. *J Mech Des* 127(6):1077–1087
- Donoho DL (2006) Compressed sensing. *IEEE Trans Inf Theory* 52(4):1289–1306
- Eldar YC, Kutyniok G (2012) Compressed sensing: theory and applications. Cambridge University Press, Cambridge
- Fang HB, Horstemeyer MF (2006) Global response approximation with radial basis functions. *Eng Optim* 38(4):407–424
- Ghanem RG, Spanos PD (1991) Stochastic finite elements: a spectral approach. Springer-Verlag, Berlin
- Gibbons JD, Chakraborti S (2014) Nonparametric statistical inference: revised and expanded. CRC Press, Boca Raton
- Goel T, Haftka RT, Wei S, Queipo NV (2007) Ensemble of surrogates. *Struct Multidiscip Optim* 33(3):199–216
- Gorissen D, Crombecq K, Hendrickx W, Dhaene T (2007) Adaptive distributed metamodeling. High Performance Computing for Computational Science (VECPAR 2006). *Lect Notes Comput Sci* 4395:579–588
- Hajikolaie KH, Wang GG (2014) High dimensional model representation with principal component analysis. *J Mech Des* 136(1):011003
- Huang ZY, Qiu HB, Zhao M, Cai XW, Gao L (2015) An adaptive SVR-HDMR model for approximating high dimensional problems. *Eng Comput* 32(3):643–667
- Hussain MF, Barton RR, Joshi SB (2002) Metamodeling: radial basis functions, versus polynomials. *Eur J Oper Res* 138(1):142–154
- Ishigami T, Homma T (1990) An importance quantification technique in uncertainty analysis for computer models. Proceedings of the First International Symposium on Uncertainty Modeling and Analysis (ISUMA'90), University of Maryland, 398–403. <https://doi.org/10.1109/ISUMA.1990.151285>
- Jin R, Chen W, Simpson TW (2001) Comparative studies of metamodeling techniques under multiple modelling criteria. *Struct Multidiscip Optim* 23(1):1–13
- Johnson ME, Moore LM, Ylvisaker D (1990) Minimax and maximum distance designs. *J Stat Plan Infer* 26(2):131–148
- Jones DR, Perttunen CD, Stuckman BE (1993) Lipschitzian optimization without the Lipschitz constant. *J Optim Theory Appl* 79(1):157–181
- Kenett R, Zacks S (1998) Modern industrial statistics: design and control of quality and reliability. Duxbury Press, Belmont
- Lee SH, Chen W (2009) A comparative study of uncertainty propagation methods for black-box-type problems. *Struct Multidiscip Optim* 37(3):239–253
- Li EY, Wang H (2016) An alternative adaptive differential evolutionary algorithm assisted by expected improvement criterion and cut-HDMR expansion and its application in time-based sheet forming design. *Adv Eng Softw* 97:96–107
- Li GY, Rosenthal C, Rabitz H (2001) High dimensional model representations. *J Phys Chem A* 105(33):7765–7777
- Li GY, Hu JS, Wang SW, Georgopoulos PG, Schoendorf J, Rabitz H (2006) Random sampling-high dimensional model representation (RS-HDMR) and orthogonality of its different order component functions. *J Phys Chem A* 110(7):2474–2485
- Li YF, Ng SH, Xie M, Goh TN (2010) A systematic comparison of metamodeling techniques for simulation optimization in decision support systems. *Appl Soft Comput* 10(4):1257–1273
- Li EY, Ye F, Wang H (2017) Alternative Kriging-HDMR optimization method with expected improvement sampling strategy. *Eng Comput* 34(6):1807–1828
- Liu HT, Hervas JR, Ong YS, Cai JF, Wang Y (2018) An adaptive RBF-HDMR modeling approach under limited computational budget. *Struct Multidiscip Optim* 57(3):1233–1250
- Martin JD, Simpson TW (2005) Use of kriging models to approximate deterministic computer models. *AIAA J* 43(4):853–863
- Mukhopadhyay T, Dey TK, Chowdhury R, Chakrabarti A, Adhikari S (2015) Optimum design of FRP bridge deck: an efficient RS-HDMR based approach. *Struct Multidiscip Optim* 52(3):459–477
- Ostergard T, Jensen RL, Maagaard SE (2018) A comparison of six metamodeling techniques applied to building performance simulations. *Appl Energy* 211:89–103
- Parnianifard A, Azfanizam AS, Ariffin MKA, Ismail MIS (2020) Comparative study of metamodeling and sampling design for expensive and semi-expensive simulation models under uncertainty. *Simulation* 96(1):89–110
- Rabitz H, Alis OF (1999) General foundations of high-dimensional model representations. *J Math Chem* 25(2–3):197–233
- Rabitz H, Alis OF, Shorter J, Shim K (1999) Efficient input-output model representations. *Comput Phys Commun* 117(1–2):11–20
- Shan SQ, Wang GG (2010a) Metamodeling for high dimensional simulation-based design problems. *J Mech Des* 132(5):051009
- Shan SQ, Wang GG (2010b) Survey of modeling and optimization strategies to solve high-dimensional design problems with computationally-expensive black-box functions. *Struct Multidiscip Optim* 41(2):219–241
- Shan SQ, Wang GG (2011) Turning black-box functions into white functions. *J Mech Des* 133(3):031003
- Sobol IM (1993) Sensitivity estimates for nonlinear mathematical models. *Math Model Comput Exp* 1(4):407–414
- Sudret B (2008) Global sensitivity analysis using polynomial chaos expansions. *Reliab Eng Syst Saf* 93(7):964–979
- Szepietowska K, Magnain B, Lubowiecka I, Florentin E (2018) Sensitivity analysis based on non-intrusive regression-based polynomial chaos expansion for surgical mesh modelling. *Struct Multidiscip Optim* 57(3):1391–1409
- Tang L, Wang H, Li GY (2013) Advanced high strength steel springback optimization by projection-based heuristic global search algorithm. *Mater Des* 43:426–437
- Thomas PS, Somers MF, Hoekstra AW, Kroes GJ (2012) Chebyshev high-dimensional model representation (Chebyshev-HDMR) potentials: application to reactive scattering of H₂ from Pt(111) and Cu(111) surfaces. *Phys Chem Chem Phys* 14(24):8628–8643
- Tropp JA, Gilbert AC (2007) Signal recovery from random measurements via orthogonal matching pursuit. *IEEE Trans Inf Theory* 53(12):4655–4666
- Tunga MA (2011) An approximation method to model multivariate interpolation problems: indexing HDMR. *Math Comput Model* 53(9–10):1970–1982
- Tunga MA, Demiralp M (2006) Hybrid high dimensional model representation (HHDMR) on the partitioned data. *J Comput Appl Math* 185(1):107–132
- Van Gelder L, Das P, Janssen H, Roels S (2014) Comparative study of metamodeling techniques in building energy simulation: guidelines for practitioners. *Simul Model Pract Theory* 49:245–257
- Wang H, Tang L, Li GY (2011) Adaptive MLS-HDMR metamodeling techniques for high dimensional problems. *Expert Syst Appl* 38(11):14117–14126
- Wang H, Chen LM, Ye F, Chen L (2017) Global sensitivity analysis for fiber reinforced composite fiber path based on D-MORPH-HDMR algorithm. *Struct Multidiscip Optim* 56(3):697–712
- Xie SJ, Pan BS, Du XP (2017) High dimensional model representation for hybrid reliability analysis with dependent interval variables constrained within ellipsoids. *Struct Multidiscip Optim* 56(6):1493–1505
- Xiu D, Karniadakis GE (2002) The Wiener-Askey polynomial chaos for stochastic differential equations. *SIAM J Sci Comput* 24(2):619–644
- Xu SL, Liu HT, Wang XF, Jiang XM (2014) A robust error-pursuing sequential sampling approach for global metamodeling based on Voronoi diagram and cross validation. *J Mech Des* 136(7):071009

- Yang QW, Xue DY (2015) Comparative study on influencing factors in adaptive metamodeling. *Eng Comput* 31(3):561–577
- Zeng P (2009) *Fundamentals of finite element analysis*. Higher Education Press, Beijing
- Zhang N, Wang P, Dong HC (2019) Research on high-dimensional model representation with various metamodels. *Eng Optim* 51(8):1336–1351
- Zhang J, Yue XX, Qiu JJ, Zhang MY, Wang XM (2021a) A unified ensemble of surrogates with global and local measures for global metamodeling. *Eng Optim* 53(3):474–495
- Zhang J, Yue XX, Qiu JJ, Zhuo LJ, Zhu JG (2021b) Sparse polynomial chaos expansion based on Bregman-iterative greedy coordinate descent for global sensitivity analysis. *Mech Syst Signal Process* (in press)

Publisher's note Springer Nature remains neutral with regard to jurisdictional claims in published maps and institutional affiliations.